The impact of energy prices on the electrification of utility systems in industries with fluctuating energy demand

Bielefeld, Svenja; de Raad, Brendon; Stougie, Lydia; Cvetković, Miloš; Lieshout, Marit van; Ramírez, Andrea

DOI
10.1016/j.energy.2025.137679

Publication date
2025

Document Version
Final published version

Published in
Energy

Citation (APA)
Bielefeld, S., de Raad, B., Stougie, L., Cvetković, M., Lieshout, M. V., & Ramírez, A. (2025). The impact of energy prices on the electrification of utility systems in industries with fluctuating energy demand. *Energy*, *335*, Article 137679. https://doi.org/10.1016/j.energy.2025.137679

Energy 335 (2025) 137679

Contents lists available at ScienceDirect

Energy

journal homepage: www.elsevier.com/locate/energy

The impact of energy prices on the electrification of utility systems in industries with fluctuating energy demand

Svenja Bielefeld [a,*], Brendon de Raad [a,b], Lydia Stougie [a], Miloš Cvetković [c], Marit van Lieshout [b], Andrea Ramírez [d]

[a] Engineering Systems and Services Department, Faculty of Technology, Policy and Management, Delft University of Technology, The Netherlands
[b] Rotterdam University of Applied Sciences, Rotterdam, The Netherlands
[c] Electrical Sustainable Energy Department, Faculty of Electrical Engineering, Mathematics & Computer Science, Delft University of Technology, The Netherlands
[d] Department of Chemical Engineering, Faculty of Applied Science, Delft University of Technology, The Netherlands

ARTICLE INFO

Dataset link: https://github.com/SvenjaBie/ElectrUtilPapInd_Open

Keywords:
Electrification
Energy-intensive industry
Flexibility
Optimisation
Power-to-heat technologies
Energy storage

ABSTRACT

Industrial greenhouse gas emissions, primarily carbon dioxide, constitute about one-third of global emissions, and 75% are caused by the generation of heat from fossil fuels. Therefore, a key decarbonisation strategy is electrifying heat generation using renewable sources and power-to-heat technologies. This study explores the impact of the energy price on the optimal choice and sizing of power-to-heat and storage technologies in existing energy-intensive industries with a variable heat demand. A mixed integer linear program is used to determine the technology portfolio and size of the equipment that leads to the lowest total annual cost of the utility system while ensuring that heat demand is always fulfilled. The results of a case study in the Netherlands show that adding power-to-heat and storage technologies to a fossil fuel-based combined heat and power plant is economically viable under all explored scenarios. The mean and the variance of electricity prices significantly influence the sizing of heat pumps, electric boilers, and thermal energy storage. High and stable electricity prices lead to larger heat pump capacities compared to scenarios with low and more variable electricity prices. Electric boilers are primarily sized based on the variance of electricity prices and the capacity of thermal energy storage, which plays a crucial role in managing electricity price fluctuations. The study emphasises the potential for cost-effective electrification and provides valuable insights for reducing industrial CO_2 emissions.

1. Introduction

International commitments aim to reduce greenhouse gas (GHG) emissions significantly [1]. Approximately one-third of global GHG emissions stem from the industry and consist mainly of CO_2 emissions [2]. Roughly 75% of these emissions are related to the combustion of fossil fuels for fulfilling heating requirements [3]. Therefore, electrifying heat generation with renewable sources is considered a key pathway to reducing industrial CO_2 emissions [4].

Power-to-heat (PtH) technologies have gained attention as they can (a) directly convert electrical power into heat (using, e.g., an electric boiler (ElB)), (b) use electrical power to produce an intermediate energy carrier, such as hydrogen (H2), that can be stored and thereafter converted into heat, or (c) use electrical power to upgrade waste heat streams (with, e.g., a heat pump (HP)) [5]. Among the three options, waste heat-upgrading technologies such as heat pumps require the least electricity to generate heat [6]. Yet, the technical performance of a heat pump is highly dependent on the temperature at which heat is demanded and available [7].

Combining PtH technologies with energy storage can increase the use of renewable electricity, reduce CO_2 emissions and improve the economic performance of an industrial plant's energy conversion facility (utility system), as they enable energy use when it is abundant and cheap [8]. However, identifying cost-effective combinations of PtH and storage technologies is challenging due to varying and uncertain equipment costs and efficiencies, as well as the fluctuating availability and cost of renewable electricity.

This challenge has been studied from different perspectives in the literature, and studies can be categorised into three groups. The first compares different PtH technologies with each other in scenarios with a constant energy price, excluding the option of energy storage. Son et al. [5], for example, study the potential role of PtH technologies in an oil refinery with a pinch analysis and identify economically feasible

* Corresponding author.
E-mail address: s.e.bielefeld@tudelft.nl (S. Bielefeld).

https://doi.org/10.1016/j.energy.2025.137679
Received 3 April 2025; Received in revised form 27 June 2025; Accepted 19 July 2025
Available online 23 August 2025

HP and ElB solutions. Wiertzema et al. used the same approach to study the impact of electrifying the utility system on the heat integration of a chemical process and found that replacing a gas boiler with an electric boiler reduces the waste heat and therefore the potential for heat integration. However, they also found that the operational cost of the selected electric boiler halved in 2040, compared to a 2030 energy market scenario [9]. Kim et al. used pinch analysis at the site level and found several electrification options, but excluded an assessment of their economic performance [10]. Walden and Stathapopoulos used a time-sliced pinch approach to study the impact of a fluctuating heat demand on the optimal integration of a heat pump and found that a heat pump can provide flexibility up to a point at which part-load behaviour leads to diminishing returns [11].

The second group of studies considers fluctuating energy prices, but explores the use of only one PtH and storage technology. Walden et al. [12], for example, used optimisation to study the operation of a high temperature heat pump and a sensible thermal energy storage with electricity coming from the power grid and a wind turbine in a process with a constant heat demand. Trevisan et al. used mixed integer linear optimisation to study the techno-economic feasibility of molten salt-based thermal energy storage with embedded electrical heaters for a process with a variable heat demand and different electricity spot market prices [13].

The third group considers multiple PtH and storage technologies and fluctuating energy prices. Baumgaertner et al. [14], for example, studied the impact of time-dependent grid emissions on the design and operation of an electrified utility system with a mixed integer linear model for a pharmaceutical facility with a fluctuating energy demand. While they include varying electricity prices in their study, the gas price is kept constant. Reinert et al. [15] expanded this work and added the possibility of pumped thermal energy storage. However, again, gas prices were kept constant. Previous work by some of the authors of this study explored the potential for cost-optimal electrification of existing utility systems for chemical plants with fluctuating electricity and gas prices. Direct and indirect electrification with electric and hydrogen boilers was considered, but the option to upgrade waste heat with a heat pump was not included [16]. Fleschutz et al. [17] studied using the combination of an ElB, hydrogen as an energy carrier, a heat pump and forms of energy storage for electrification for industrial applications. However, the assessment was carried out for low-temperature heat requirements, for which the performance of the heat pump is significantly different from the performance in the case of high-temperature applications.

The studies presented thus far do not analyse the impact of energy price profiles on the combination of PtH and storage technologies under fluctuating energy prices and operational conditions for existing high-temperature industrial applications. Insight into the potential role of electrification technologies under these circumstances is needed to enable cost-effective electrification of current fossil industrial heating systems.

The aim of this work is thus to evaluate the impact of variable energy prices on deploying PtH and storage technologies in an energy-intensive industry with variable high-temperature heat demand and existing heating infrastructure. Herein, the trade-off between options with a higher efficiency and a higher cost, i.e., heat pumps, and options with lower efficiency and cost, i.e., electric boilers, is explored. The contribution to the existing literature on electrified utility systems for industrial plants is twofold.

1. This work presents a feasibility assessment of technology portfolios that enable cost-effective electrification of fluctuating high-temperature heat demand requiring minimal changes to the plant's existing infrastructure.
2. The impact of the mean and variance of energy prices and the electricity to gas price-ratio on the selection and sizing of technologies, specifically on heat pumps, is shown.

2. Methods

This section introduces the existing utility system and potential investment options (Section 2.1), describes the model used to design and simulate the cost-optimal utility system (Section 2.2) and presents the case study (Section 2.3). Thereafter, the reference utility system and the explored scenarios are described (Sections 2.4 and 2.5).

2.1. Existing utility system and potential investment options

The model used to design and assess cost-optimal electrified utility systems is based on an existing utility system fuelled by natural gas (NG). This system, shown in Fig. 1, comprises a bidirectional connection to the local power grid, a gas-fired gas turbine (GT) and a heat recovery steam generator (HRSG) with additional natural gas co-firing in a gas boiler (GB). The co-firing allows additional heat generation without producing power and enables the system to react to fluctuations in process heat demand. The GT, HRSG, and GB are referred to as combined heat and power plant (CHP) for the remainder of this paper. Since the CHP has already been installed, it is assumed that it does not require further investments. Investments due to maintenance are also not included.

To electrify the utility system, PtH technologies and storage technologies can be added to the system as shown in Fig. 2. The PtH technologies considered in this study include an HP, which utilises excess heat from a heat recovery unit, an electric boiler (ElB), and a hydrogen boiler (H2B) fuelled with hydrogen generated by a proton exchange membrane water electrolyser (H2E). The decision to include hydrogen is based on low-cost storage opportunities in hydrogen tanks (see Table 5). The storage units considered are a Li-Ion battery (Bat), a sensible TES and a hydrogen storage tank (H2S). Due to the different temperature levels at which the PtH technologies produce heat, in practice, they would not be connected to the same TES unit. To reduce complexity, the TES is considered one unit in the model. Furthermore, it is assumed that the HP and the TES produce heat at the temperature required by the process and that the heat from the ElB is cascaded down to the required level by using throttling valves. The cost of these valves is not included in the model as it is considered minor compared to the cost of the PtH and storage equipment.

2.2. Model formulation

This work explores how changes in the electricity price affect the technology portfolio and economic performance of the system. Deterministic optimisation in combination with scenario analysis is used, as the paper does not aim to find the best solution for all uncertain parameters but rather to understand the model's response to them. The model is implemented using the Python-based optimisation package 'Pyomo' and solved using Gurobi solvers. Its time resolution is $\Delta t = 0.5\ h$, following the resolution of the demand data of the case study. The solving time depends on the scenario. Some scenarios could not be solved to full optimality on a laptop (with Intel CORE i7 vPRO processor) and had to be solved on a supercomputing cluster. The default optimality gap was set to 0.005%.

The model departs from a model presented in [16] and was extended to include an HP and a more flexible CHP. The objective of the optimisation is to minimise the total cost of the utility system for the duration of one operational year, including the investment cost (CapEx) and the operational costs (OpEx), see Eq. (D.11). Since the model runs in half-hourly steps and the operational time of the process is 8000 h, assuming 760 h of downtime per year, the model includes 16000 time steps.

$$min \sum_{t=0}^{t=16000} \mathrm{OpEx}(t) + \mathrm{CaPex} \tag{1}$$

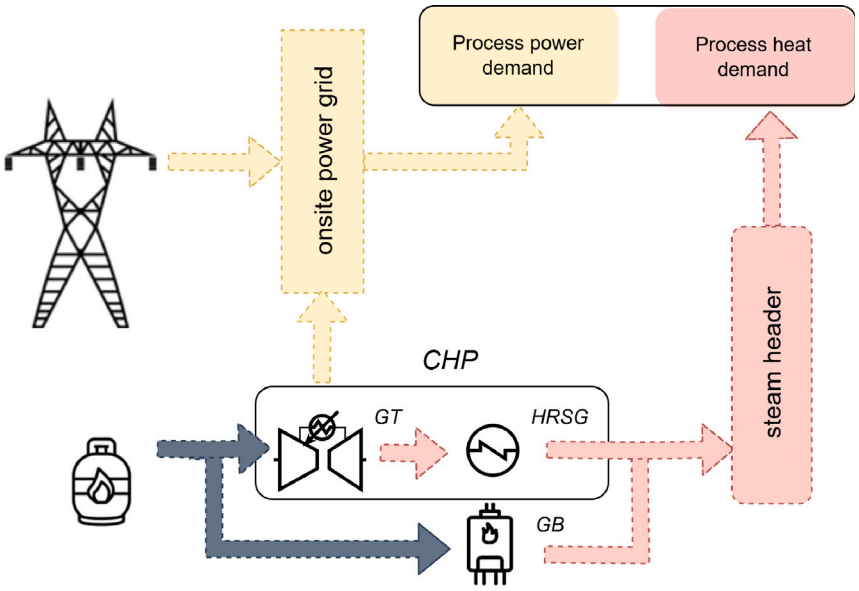

Fig. 1. Fossil fuel-based utility system assumed to be the existing utility system for the plant considered in this study. Note that the onsite power grid and steam header are added to the figure for better readability, but are not included in the model. The heat demand is supplied by a CHP, which consists of a gas turbine (GT) and a heat recovery steam generator (HRSG) with additional natural gas co-firing in a gas boiler (GB). The power demand is supplied by the power produced by the GT or by electricity from the national power grid.

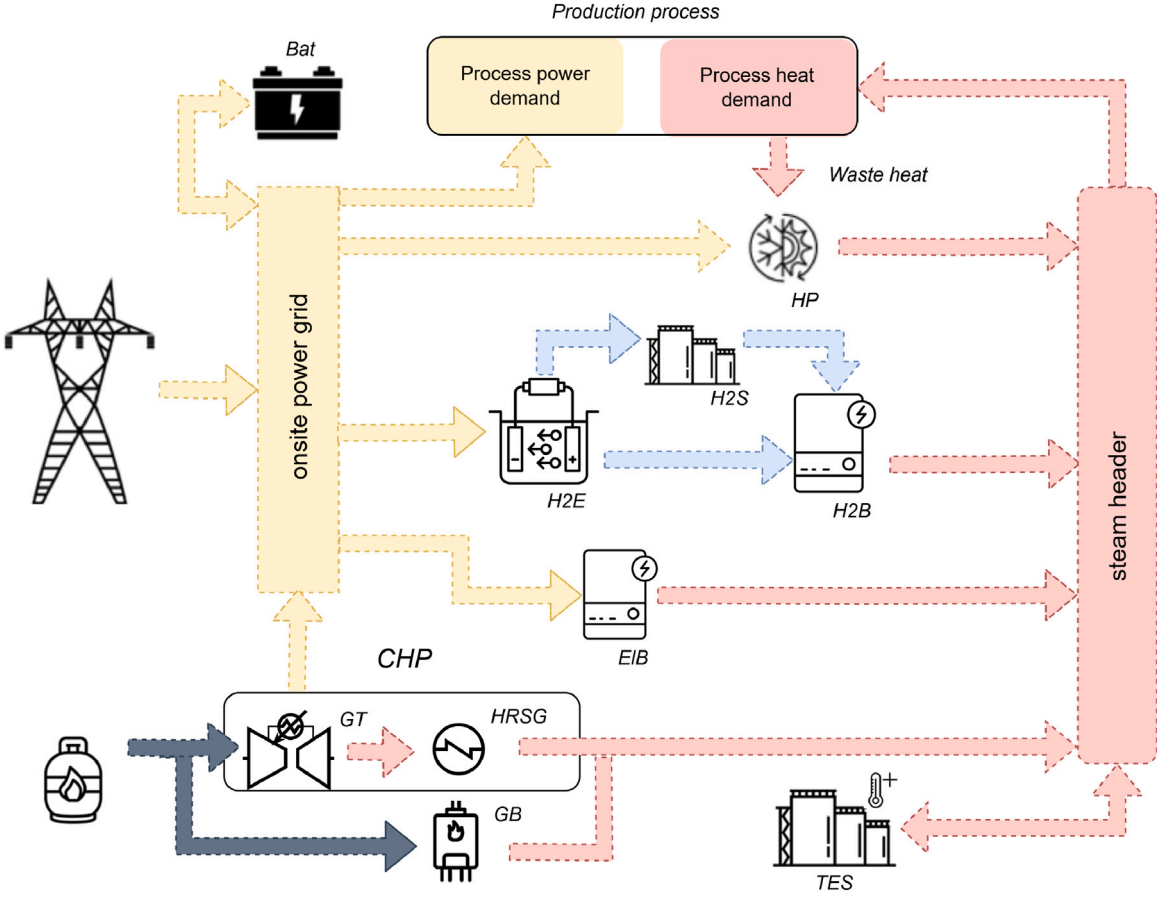

Fig. 2. Potential utility system design including a fossil-based legacy utility system (CHP) consisting of a gas turbine (GT) with a heat recovery steam generator (HRSG) and a gas boiler (GB), and an electric boiler (ELB), a heat pump (HP), and a power-to-gas-to-heat system consisting of an electrolyser (H2E), a hydrogen storage tank (H2S), and a hydrogen boiler (H2B). Energy can be stored in batteries (Bat) and thermal energy storage (TES). Note that the onsite power grid and steam header are used to improve the visualisation. In the model, all interconnections between technologies and from the technologies to the gas or power grid are modelled separately.

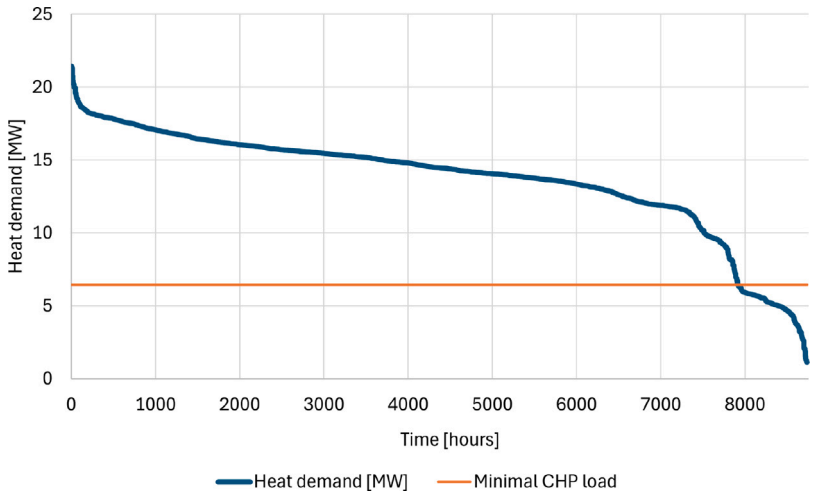

Fig. 3. Heat demand duration curve of the process in the case study and the demand that the CHP supplies at its minimal possible load.

The OpEx is calculated using Eq. (2). It consists of the cost of consuming grid electricity minus the potential revenue from selling electricity from the CHP back to the grid and the cost of consuming natural gas (including the cost of purchasing CO_2 emission allowances within the European Emission Trading System (EU ETS)). Taxes and other fees for selling power back to the grid are not included in the model. In Eq. (2), $p_{el,\ grid}(t)$ is the electricity price at time t in [euro/MWh]. Power flow from the grid to technology i is denoted as $P_{gr,i}(t)$ and power flow from technology i back to the grid as $P_{i,gr}(t)$. Both are expressed in [MW]. $p_{NG}(t)$ is the cost of using natural gas at time t in [euro/MWh]. The quantity of gas consumed per time step is denoted by $NG_{in}(t)$ in [MW].

$$\mathrm{OpEx}(t) = p_{el,\ grid}(t) \cdot \sum (P_{gr,i}(t) - P_{i,gr}(t)) \cdot \Delta t + p_{NG}(t) \cdot NG_{in}(t) \cdot \Delta t \quad (2)$$

The CapEx (Eq. (3)) includes the investment required for all newly installed technologies i and is a product of their technology cost c_i (in [euro/MW] or [euro/MWh]), their installation factor Inf_i and their size s_i (in [MW] or [MWh]).

$$\mathrm{CaPex} = \sum_i c_i \cdot \mathrm{Inf}_i \cdot s_i \cdot \mathrm{AF}_i \quad (3)$$

Since the model only considers one operational year, the investment is annualised using an annualisation factor of the respective technology AF_i, which is calculated using Eq. (4). LT_i is the lifetime of equipment i, and the discount rate r is set to 10%, as in [17].

$$\mathrm{AF}_i = \frac{r}{1-(1+r)^{-LT_i}} \quad (4)$$

The power or heat generation and storage technologies are represented by energy flow balances and the respective technological constraints, as described in section 2.1 of [16]. The CHP in this study is modelled as a combination of a gas turbine, a heat recovery steam generator, and a gas boiler. Mirroring the situation of the case study, the operational flexibility of the GT is based on the combined operation of two gas turbines, which both have the ability to operate at 60%–100% of their capacity. It is assumed that one turbine can be shut down completely. One GT, or 30% of the total GT thermal output, has to operate at all times to limit the number of cold starts, which damage the equipment. Therefore, the minimal load of the CHP is assumed to be 30% of its capacity. The heat generation of the CHP is calculated using Eq. (5), where $NG_{GT,in}(t)$ is the amount of natural gas converted in the gas turbine, $\eta_{GT,th}$ the thermal conversion efficiency of the gas turbine, $NG_{GB,in}(t)$ the amount of natural gas going to the gas boiler, η_{GB} the conversion efficiency of the gas boiler and $H_{CHP,out}(t)$ the heat output of the CHP.

$$\left(NG_{GT,in}(t) \cdot \eta_{GT,th} + NG_{GB,in}(t)\right) \cdot \eta_{GB} = H_{CHP,out}(t) \quad (5)$$

The energy conversion of the HP is modelled as stated in Eq. (6), where $H_{HP,out}(t)$ is the heat output of the HP, which is a function of the power input $P_{HP,in}(t)$ and the ideal, or Carnot, coefficient of performance (COP) COP_{ideal} multiplied by 0.5 because a mechanical closed-cycle HP is expected to operate at 50% of its ideal COP [18,19].

$$H_{HP,out}(t) = P_{HP,in}(t) \cdot \mathrm{COP}_{ideal} \cdot 0.5 \quad (6)$$

The ideal COP is calculated using Eq. (7).

$$\mathrm{COP}_{ideal} = T_{sink}/(T_{sink} - T_{source}) \quad (7)$$

All equations of the model are presented in Appendix D.

2.3. Case study

This study explores the electrification of the utility supply for the energy-intensive industry with a highly fluctuating electricity and (high-temperature) heat demand. These conditions are commonly observed in sectors with a large product portfolio, batch processing, and or cleaning-in-place processes such as in the food and beverage, the chemical and pharmaceutical, the textile and the paper and pulp industry. An existing paper mill in the Netherlands with various paper recipes is used as a representative case study for this group of discontinuous processes.

Of the considered paper mill, only the heat demand of the drying section was considered, as it requires over 80% of the total heat demand. The heat demand, between 100 °C and 160 °C, varies in capacity every 30 minutes. The maximum heat demand is 21.5 MW, the average 13.7 MW and the minimum 1.1 MW. Fig. 3 shows the demand duration curve of the process (in blue) and the heat delivered by the CHP when it operates at its minimal load (in orange). For confidentiality reasons, a more detailed description of the underlying demand data cannot be disclosed.

Excess heat can be recovered from the drying hood at $T = 55$ °C and fed to a HP. Since the HP is required to generate heat at 160 °C, the COP of the HP for this paper mill is 2 based on a second law efficiency of 50%. The electricity demand is assumed to be 10% of the heat demand based on information obtained from the plant operator. The grid connection capacity that limits the power flow from or to the local power grid was assumed to be 30 MW based on the capacity of the actual grid connection of the case study plant.

Table 1
Data used to model conversion technologies.

	Gas turbine	Gas boiler	ElB	HP	Electrol-yser	H2 boiler
Capacity						
thermal [MW_{th}]	$H_{dem,max}/\eta_{GB}$	20% of GT	decision variable	decision variable	decision variable	decision variable
electric [MW_{el}]						
Efficiency η [%]	$\eta_{thermal} = 60$, $\eta_{el} = 30$[a]	82	99 [21,22]	$0.5 \cdot COP_{ideal}$	69 [23]	92 [24,25]
Minimal load factor [% of max. load]	0.5 ·60	0	0	0	0	
Lifetime LT [years]	not included in model		20 [22]	20 [7]	15	20 [26]

[a] Note that $\eta_{thermal}$ concerns the generation of heat from natural gas

Table 2
Data used to model storage technologies.

	Battery	TES	Hydrogen tank
Capacity	decision variable	decision variable	decision variable
Efficiency η [%]	90 [17]	90 [27]	90 [17]
Maximum energy output [% of capacity/Δt]	70 [17]	50 [17]	100
Lifetime LT [years]	15 [28]	25 [29]	20 [30]

2.3.1. Technical parameters

The parameters used to model the technologies are shown in Tables 1 and 2. Except for the minimal load factor of the CHP, the data is derived from literature. The minimal load factor of the gas turbine is dictated by the equipment installed in the paper mill, and in line with the proposed 50% operational flexibility by Voll et al. [20]. Appendix C shows how the results would look like for more flexible CHPs.

2.4. Reference utility system

The fossil fuel-based legacy utility system described in 2.1 is the reference system of this study. The reference system's total cost is its operational cost, which is calculated according to the cost-optimal operation of the system as described in Eq. (8). The total cost of the reference system is the sum of the costs for grid power and NG use. The cost for grid power use is a function of the electricity price at time t and the difference between electricity consumed by the process $P_{gr,process}(t)$ minus the power generated by the GT and sold to the grid, $P_{GT,gr}(t)$. The cost for NG consumption is a function of the natural gas price at t and the gas used by the gas turbine and the boiler, $NG_{GT,in}(t)$ and $NG_{GB,in}(t)$.

$$\text{Total Cost} = min \sum_{t=0}^{t=16000} \Big(p_{el,\ grid}(t) \cdot \Delta t \cdot \big(P_{gr,process}(t) - P_{GT,gr}(t) \big) + p_{NG}(t) \cdot \Delta t \cdot \big(NG_{GT,in}(t) + NG_{GB,in}(t) \big) \Big) \quad (8)$$

The same technical parameters and constraints are used as in the optimisation model described in 2.2. All equations used are shown in Appendix D.2.

2.5. Scenarios with differing techno-economic assumptions

The optimisation model is run for a number of energy price scenarios and technology cost (TC) scenarios since the design of an electrified utility system depends on capital and operational costs, and both are subject to uncertainties. The scenario tree containing all explored scenarios is included in the Appendix (Fig. A.15).

2.5.1. Energy price scenarios

Three uncertainties have been addressed in this paper, namely (1) The average energy price because of the trade-off between investment and operational cost, (2) energy price variability because of the potential value of flexibility in the utility system, and (3) the electricity-to-gas price ratio (EGR) because PtH technologies compete with existing gas-based technologies. To understand the impact of these uncertainties, several energy price scenarios were designed.

The average electricity price for the 'low mean' scenario is 30 euro/MWh and is based on the average price of electricity on the Dutch day-ahead market in 2020 [31]. The mean electricity price of the 'high mean' scenario is 100 euro/1u MWh and is based on 2023 data from the same market [31]. The electricity price volatility (its variance) is included via two scenarios, i.e. with a low variance, based on 2019 data, and with a high variance, based on 2023 (Dutch day-ahead market) data [31]. A combination of the two mean and the two variance scenarios leads to four electricity price scenarios. The abbreviations used in the first column of Tables 3 and 4 are based on the mean price and the level of price variance of the respective scenario. The scenario with a low mean price and high levels of price variance, for example, is named 'LMHV' ('Low Mean High Variance').

Two gas price scenarios are added to each electricity price scenario to explore the impact of the EGR. One scenario has cheaper gas than electricity prices, based on the average EGR (including EU ETS allowance price) in 2023 of 1.6 (see data in [31–33]). Note that companies in the Netherlands did not have to pay for all of their CO_2 emissions and that including free allocation rights would result in an EGR of > 2 in 2023. For the second scenario, an EGR of 1 was assumed to simulate scenarios with increased gas use prices. The gas price profiles are based on Dutch TTF market data [32] and were adapted to have a mean price matching the desired EGR. To avoid negative gas prices, the gas price is capped at 10 euro/MWh, which aligns with the lowest price in the period 2021 to 2024 (see data in [32,34]). 17 euro/MWh_{NG} (85 euro/ton_{CO_2}) are added to the gas price, mimicking prices in 2023, to include the cost of purchasing CO_2 emission certificates to the cost of using natural gas [35]. This CO_2 price is used in all gas price scenarios.

Tables 3 and 4 provide information about the resulting price scenarios. All price profiles are shown in Figs. A.11 to A.14 in Appendix A.

Table 3
Electricity price and negative price statistics in the energy price scenarios.

Scenario	EGR	Electricity Price		Negative Prices	
		Mean (Euro/MWh)	Variance (Euro/MWh)^2	Number of hours	Average Value (Euro/MWh)
LMLV	1.6	30	127	30	−6.82
	1	30	127	30	−6.82
LMHV	1.6	30	2,405	1,641	−43.67
	1	30	2,405	1,641	−43.67
HMLV	1.6	100	127	–	–
	1	100	127	–	–
HMHV	1.6	100	2,405	155	−47.46
	1	100	2,405	155	−47.46

Table 4
Natural gas use cost and hours when the electricity price is lower than the gas cost (including the price for emitting CO_2).

Scenario	EGR	Natural Gas Use Cost		Electricity Price < Gas Cost
		Mean (Euro/MWh)	Variance (Euro/MWh)^2	Number of hours
LMLV	1.6	35.75	10	6,649
	1	47	10	8,269
LMHV	1.6	35.75	113	4,431
	1	47	113	5,814
HMLV	1.6	79.5	10	121
	1	117	10	8,269
HMHV	1.6	79.5	113	1,945
	1	117	113	5,816

Table 5
Technology cost scenarios.

Technology	Technology cost per scenario		Reference	Lang Factor
	'HighHP-LowRest'	'LowHP-HighRest'		
ElB	60 euro/kW	60 euro/kW	[22]	1
HP	500 euro/kW	300 euro/kW	[7]	3
Battery	180 euro/kWh	320 euro/kWh	[28]	2.5
Thermal Energy Storage	15 euro/kWh	40 euro/kWh	[37]	2.5
Electrolyser	760 euro/kW	980 euro/kW	[23,38]	1
Hydrogen boiler	35 euro/kW	35 euro/kW	[26]	2
Hydrogen storage	10 euro/kWh	10 euro/kWh	[27]	4

2.5.2. Technology cost scenarios

In this study, the cost for new equipment is the product of the technology cost and its installation cost factor. The technology cost was based on a literature review and is shown in Table 5. The installation cost factors were taken from Sinnot and Towler [36]. HPs were considered to be a collection of compressors (2.5) and heat exchangers (3.5), storage technologies miscellaneous equipment (2.5). The hydrogen boiler was considered a gas-fired boiler (2), and the hydrogen storage a pressure vessel (4). For the ElB and the electrolyser, a factor of 1 was used as the technology cost was derived from a reference, which had already included the installation cost.

Two technology cost scenarios (TC scenarios) are explored to account for the uncertainty of the TC of Bat, TES, H2E and HP. The technology cost of the ElB, the H2B and the H2S were kept the same for both the high- and low technology cost scenarios, as these technologies are mature and less price development is expected than for the remaining technologies. The first scenario favours installing HPs by assuming low HP costs and high costs for other equipment ('LowHP-HighRest'). In the second scenario, it is the other way around, i.e. HP costs are high, and the cost of the remaining equipment is low ('HighHP-LowRest'). The ranges in technology cost deliberately span a wide range for the purpose of exploring the impact of these cost scenarios on the operation and sizing of the utility system.

3. Results and discussion

In Sections 3.1 to 3.4, the cost-optimal utility systems for the energy price scenarios are presented, and it is discussed how they differ from each other and the respective reference systems. In Section 3.5, the sizing of new equipment across scenarios is discussed.

3.1. Cost-optimal utility systems for energy price scenarios with low mean and low variance

This scenario explores the electrification of the utility system if the prices are low and have low fluctuations. Table 6 shows that, while ElB and TES are installed for all values of the EGR and TC scenarios, HPs are only installed in the 'LowHP-HighRest' scenarios. No HPs are installed in the 'HighHP-LowRest' scenario. Since the same trends in technology choice and sizing can be observed in both EGR scenarios, only the operation of the systems in the 'EGR 1.6' scenarios is discussed in detail.

In the TC scenario with high HP cost ('HighHP-LowRest'), shown in Fig. 4(a), the CHP operates 97% of the time at its minimum possible load (30% of its thermal capacity) and ramps up to full capacity only when electricity prices are higher than 3 times the average price. The power generated by the CHP is either sold to the power grid when electricity prices are high or directly fed to the paper mill (herein referred to as the process) and the ElB when electricity prices are low. The heat generated by the CHP goes to the process, and excess heat

Table 6
Installed PtH and storage capacities in the energy price scenarios with low mean and variance.

EGR	TC scenario	ElB [MW_{th}]	TES [MWh]	HP [MW_{th}]
1.6	HighHP-LowRest	14	24	0
	LowHP-HighRest	6	5	5
1	HighHP-LowRest	14	28	0
	LowHP-HighRest	6	6	5

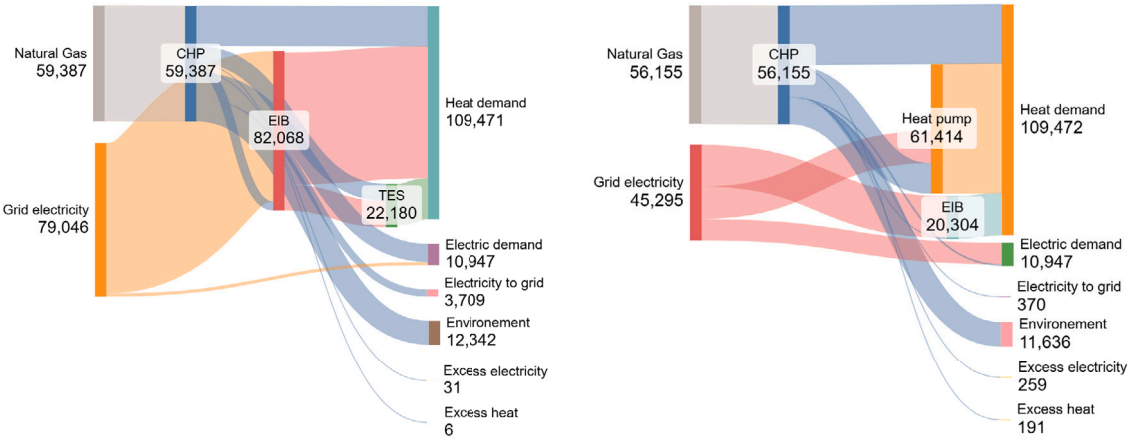

(a) TC scenario 'HighHP-LowRest' (b) TC scenario 'LowHP-HighRest'

Fig. 4. Energy exchange in [MWh] in the utility systems for the energy price scenario with low mean prices, low variance and EGR 1.6.

goes to the TES. 6% of the time, when electricity prices are very low, all energy from the CHP goes to the TES (directly or via the ElB). Power and heat are wasted (neither used nor stored) when the electricity price reaches its negative peak, to consume as much electricity as possible with the ElB. The ElB operates 68% of the time and supplies roughly 50% of the total heat demand, as Fig. 4(a) shows. It charges the TES when either heat demand is low enough and excess heat is available, electricity is cheap enough to allow for cost-effective use of the maximum capacity of the ElB, or when electricity prices are negative. Around 25% of the power for the ElB is supplied by the CHP (see Fig. 4(a)). The TES supplies heat to the process during hours with a heat demand exceeding the minimal heat output by the CHP and electricity prices that render using the ElB unfavourable.

When an HP is installed, like in the 'LowHP-HighRest' TC scenario shown in Fig. 4(b), the CHP still operates at its minimal load 97% of the time. In this scenario, the HP is the main heat supplier next to the CHP, as Fig. 4(b) shows. It operates 94% of the time, mostly at full capacity (its load factor, i.e. the total energy supplied in one operational year over the installed capacity times the number of operational hours, is 92%). Only during peak heat demand and a relatively high electricity-to-gas-price ratio, e.g., 2, is the HP turned off, and the CHP delivers all heat required by the process. This, however, only happens 3% of the time. As Fig. 4(b) shows, the CHP supplies approximately two-thirds of the power the HP requires to run and delivers almost half of the power the ElB uses. The TES supplies heat to the process at peak heat demand. It is charged mainly by the CHP and the HP. The ElB charges the TES only when electricity prices are very low, and the HP is operating at full capacity, which happens 5% of the time. The ElB operates for a similar amount of hours as in the previous scenario but contributes less to the heat demand of the process than before (compare the two diagrams in Fig. 4) as it supplies heat to the process during peak demand when the electricity prices are low, or the TES is empty. The gas boiler is used only 2% of the time and operates for two reasons. Either to supply heat demand exceeding what the ElB, TES, HP and CHP operating at minimal load combined can deliver (maximum 16 MW) and electricity prices or PtH capacities do not allow storing the additional power from the CHP, or it is used instead of the ElB when electricity prices are much higher than gas prices (e.g., 1.5 times higher).

Finally, compared to the reference utility system, less power is sold to the grid in the new systems, as Table 7 shows. The combination of PtH technologies and TES would enable an economically more efficient use of the power generated by the CHP. This is also illustrated by the reduced total use of energy (see Table 7) and the consequent cost savings.

3.2. Cost-optimal utility systems for energy price scenarios with low mean and high variance

As Table 8 shows, only ElBs and TES are installed in the scenarios with low mean and high variance energy prices. The capacities of the installed ElBs come close to the available grid connection capacity of 30 MW to exploit periods of low electricity prices. Note that the lowest price peaks are stronger than in the scenario discussed in the previous section (see 'Negative Price' column in Table 3 and Figs. A.11 to A.14). The high price variance also results in TES units from 55 to 112 MWh, a strong increase compared to the TES capacities in the scenarios in 3.1. The cost of the TES has a strong impact on its size as its capacity in the 'HighHP-LowRest' scenarios is about twice as big as in the 'LowHP-HighRest' scenarios.

Scenario 'EGR 1, HighHP-LowRest' is shown in Fig. 5 as an exemplary scenario of the energy price scenarios with low mean and high variance. The CHP operates similarly to the 'HighHP-LowRest' scenario in 3.1. The TES enables selling excess power from the CHP to the grid when electricity prices are high, while the CHP operates at its minimum possible load as the TES supplies heat to the process when the demand exceeds what the CHP can generate at minimal load. The TES is either charged by the CHP when demand is lower than the heat generated by the CHP at minimal load or by the ElB when electricity prices are low. Fig. 5 shows that the ElB is predominantly used to charge the TES. Table 9 shows that an increase in gas prices leads to a decreased use of

Table 7
Total annual cost (TAC), savings in TAC compared to the reference system, energy consumption including gas and power from the grid, and power sold to the grid in the energy price scenarios with low mean and variance.

EGR	System	TC scenario	TAC [Million euro]	TAC reduction [%]	NG to system [GWh]	Power grid to system [GWh]	System to power grid [GWh]
1.6	Ref.	–	5.9		196.5	0.02	35.1
	New	HighHP-LowRest	4.9	16.9	109.9	43.4	8.6
	New	LowHP-HighRest	4.9	16.9	107.9	21.1	3.8
1	Ref.	–	8.1		195.2	0.02	34.2
	New	HighHP-LowRest	6.1	24.7	105.3	45.7	7.2
	New	LowHP-HighRest	6.1	24.7	105	20.5	2.7

Table 8
Installed PtH and storage capacities in the energy price scenarios with low mean and high variance.

EGR	TC scenario	ElB [MW_{th}]	TES [MWh]	HP [MW_{th}]
1.6	HighHP-LowRest	29	103	0
	LowHP-HighRest	28	55	0
1	HighHP-LowRest	29	112	0
	LowHP-HighRest	28	61	0

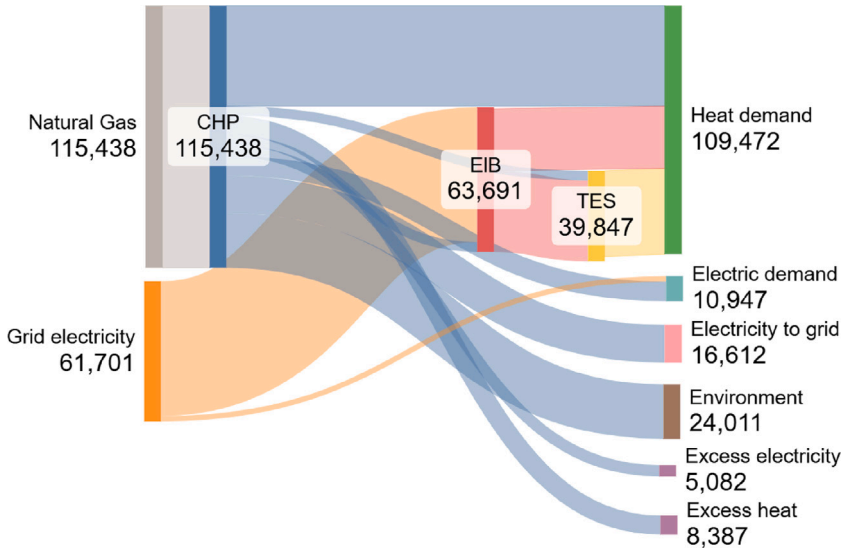

Fig. 5. Energy exchange in [MWh] in the utility systems for the energy price scenario with low mean prices, high variance, EGR 1 and TC scenario 'HighHP-LowRest'.

Table 9
Total annual cost (TAC), savings in TAC compared to the reference system, energy consumption including gas and power from the grid, and power sold to the grid in the energy price scenarios with low mean and high variance.

EGR	System	TC scenario	TAC [Million euro]	TAC reduction [%]	NG to system [GWh]	Power grid to system [GWh]	System to power grid [GWh]
1.6	Reference	–	5.4		207.1	1.9	36.4
	New	HighHP-LowRest	2.6	51.9	134.8	53.5	23.5
	New	LowHP-HighRest	3.1	42.6	139.7	50.6	24.0
1	Reference	–	7.7		201.1	1.9	32.5
	New	HighHP-LowRest	4.0	48.1	115.4	61.7	15.8
	New	LowHP-HighRest	4.5	41.6	117.5	60.2	16.6

the CHP. This explains the slightly larger TES capacities in the 'EGR 1' scenarios compared to those in the 'EGR 1.6' scenarios. The electrified utility systems lead to a higher reduction in TAC than the scenarios with a low price variance (compare Tables 7 and 9). This illustrates that the value of the flexibility to choose the energy carrier is higher than in the scenarios with lower price variance. Since ElB capacity is cheaper than HP capacity, the model chooses to install large over-capacities of ElB combined with large storage capacities to maximise the flexibility of the utility systems. Finally, more power is sold to the grid than in the scenarios with a low variance because the peaks of the electricity price profile are higher (see Table 9).

3.3. Cost-optimal utility systems for energy price scenarios with high mean and high variance

Table 10 shows the installed technologies for the scenarios with high variance and high average prices. Compared to the scenarios discussed previously, additional investments are made, and the capacities installed show larger differences between the sub-scenarios. HP

Table 10
Installed PtH and storage capacities in the energy price scenarios with high mean and high variance.

EGR	TC scenario	ElB [MW_{th}]	TES [MWh]	HP [MW_{th}]
1.6	HighHP-LowRest	31	113	2
	LowHP-HighRest	10	15	8
1	HighHP-LowRest	26	97	6
	LowHP-HighRest	9	17	9

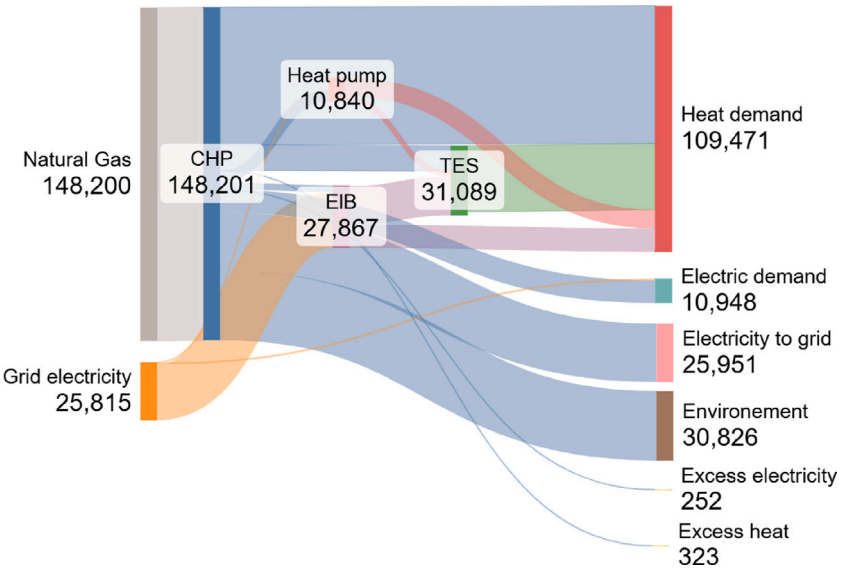

Fig. 6. Energy exchange in [MWh] in the utility systems for the energy price scenario with high mean prices, high variance, EGR 1.6 and TC scenario 'HighHP-LowRest'.

capacities range from 2 to 9 MW_{th}, TES from 15 to 113 MWh and ElB from 9 to 31 MW_{th}.

The combination of a high HP price and low gas cost in the 'EGR 1.6, HighHP-LowRest' sub-scenario results in the highest consumption of natural gas among all cost-optimal utility systems. The resulting energy flows are shown in Fig. 6. The figure shows that most electricity generated by the CHP is sold to the grid, which can be explained by the high electricity prices in this scenario (price peaks reach 470 euro/MWh), which make selling power economically more attractive than storing it in the form of heat for later use. The figure also shows that the ElB supplies more heat than the HP, unlike in other scenarios with ElB and HP instalments, such as the one shown in Fig. 4(b) in 3.1. This is because the combination of ElB and TES allows more flexibility at lower costs than a combination of HP and TES, as explained in the previous section. As a result, only a small HP of 2 MW_{th} is installed. When electricity prices are negative, the ElB operates at full capacity instead of the HP because the ElB is less efficient and consumes more electricity, which is beneficial when prices are negative.

The technology portfolio and operation of the utility system in the 'EGR 1, LowHP-HighRest' sub-scenario is very different, as Fig. 7 shows. In this scenario, the CHP delivers half of what it did in the HighHP-LowRest scenario depicted in Fig. 6, as the thermal output by the ElB doubles and that of the HP nearly triples.

The energy use across the sub-scenarios differs greatly, as shown in Table 11. Even more power is sold to the grid than in the scenario discussed in 3.2, because (mean and peak) electricity prices have increased. In the 'EGR 1.6 HighHP-LowRest' sub-scenario, this results in more power being sold to the grid than consumed. The relative savings in TAC differ by a factor of almost 2 between the EGR scenarios.

3.4. Cost-optimal utility systems for energy price scenarios with high mean and low variance

Table 12 shows that in the scenarios with high mean price and low variance, HPs and TES units are installed in all scenarios. The HP size is 8 or 9 MW, while TES capacities range from 6 to 24 MWh. ElBs are only installed in scenarios with an electricity-to-gas-price ratio of 1 and their capacity is limited to 2 MW.

The CHP operates at minimal capacity most (i.e. 95%–100%) of the time across all sub-scenarios. The heat from the CHP is fed to the process, whereas its power is used to drive the HP, the process itself and the ElB, if installed. When the process demands little heat and power, power from the CHP is sold to the grid because electricity prices are high and storage capacity is limited. The HP operates as a baseload heat supply next to the CHP, as shown for scenario 'EGR 1, HighHP-LowRest' in Fig. 8. When heat demand is low, the HP is used to charge the TES. About 8% of the time, the HP is off because the CHP alone provides enough heat. In the 'LowHP-HighRest' scenarios, HP capacity increases while the TES capacity decreases. Since the load factor of the HP in this scenario is up to 10% lower than in the scenario discussed in 3.1, this means that the HP becomes economically viable at high mean electricity prices even when it is not operated at maximum capacity throughout the year.

Table 13 shows that in all sub-scenarios, around 3 GWh are sold to the grid, which is less than in all other scenarios and less than one-tenth of the amount sold by the CHP in the reference model. This is due to the use of electricity from the CHP to power the HP. Like in the energy price scenario with high mean and variance (Section 3.3), the relative savings in TAC differ by a factor of 2 between the EGR scenarios, reflecting the difference in gas prices. This can be explained by the amount of natural gas consumed, which is relatively similar in both scenarios (see Table 13).

3.5. Equipment sizing

Fig. 9 shows the normalised equipment sizing of the ElBs, the HPs and the TESs in all considered scenarios. The small overlap between the PtH technologies shows that, in most cases, either HPs or ElBs are installed, and rarely both. Large HPs are predominantly installed in

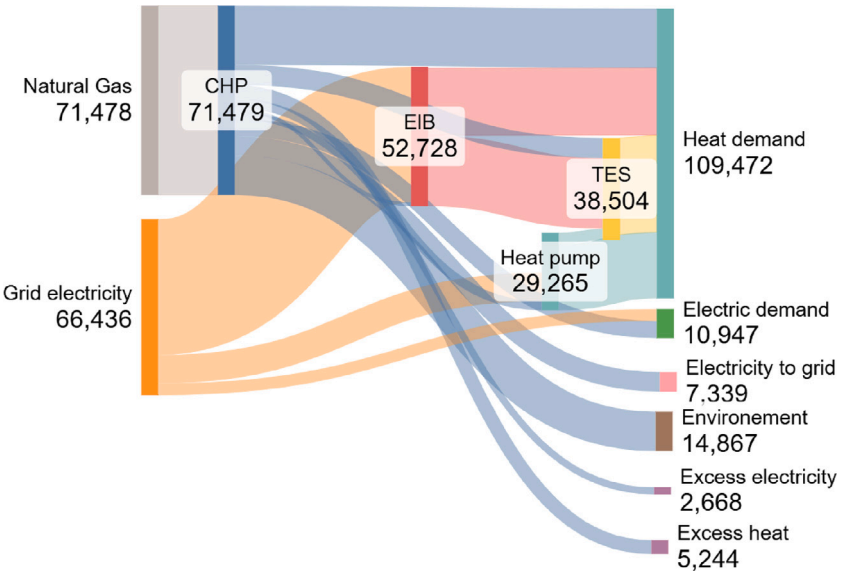

Fig. 7. Energy exchange in [MWh] in the utility systems for the energy price scenario with high mean prices, high variance, EGR 1 and TC scenario 'LowHP-HighRest'.

Table 11
Total annual cost (TAC), savings in TAC compared to the reference system, energy consumption including gas and power from the grid, and power sold to the grid in the energy price scenarios with high mean and high variance.

EGR	System	TC scenario	TAC [Million euro]	TAC reduction [%]	NG to system [GWh]	Power grid to system [GWh]	System to power grid [GWh]
1.6	Reference	–	11.8		210.5	0.2	45.0
	New	HighHP-LowRest	9.9	16.1	148.2	25.8	26.0
	New	LowHP-HighRest	9.9	16.1	121.0	11.3	26.0
1	Reference	–	19.4		196.8	0.2	34.8
	New	HighHP-LowRest	14.2	26.8	105.5	22.0	3.7
	New	LowHP-HighRest	14.0	27.8	105.2	14.7	4.1

Table 12
Installed PtH and storage capacities in the energy price scenarios with high mean and low variance.

EGR	TC scenario	ElB [MW_{th}]	TES [MWh]	HP [MW_{th}]
1.6	HighHP-LowRest	0	19	8
	LowHP-HighRest	0	6	9
1	HighHP-LowRest	2	24	8
	LowHP-HighRest	2	7	9

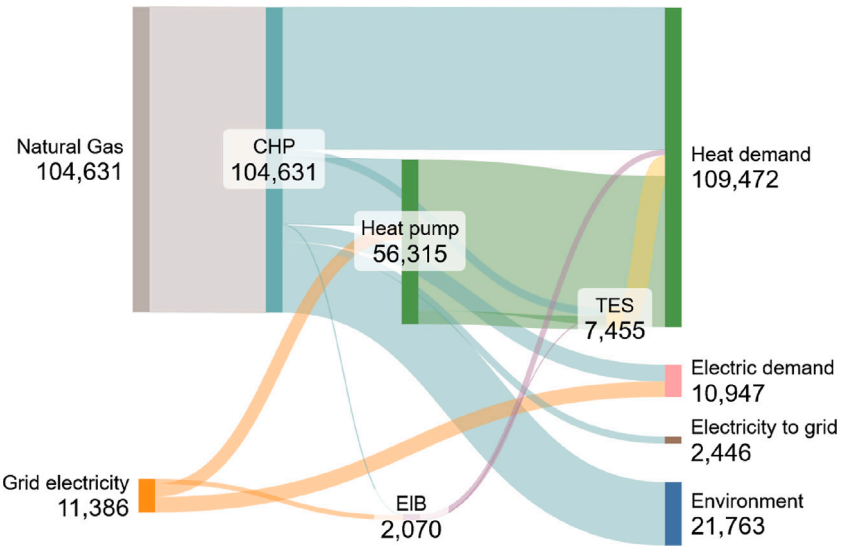

Fig. 8. Energy exchange in [MWh] in the utility systems for the energy price scenario with high mean prices, low variance, EGR 1 and TC scenario 'HighHP-LowRest'.

Table 13
Total annual cost (TAC), savings in TAC compared to the reference system, energy consumption including gas and power from the grid, and power sold to the grid in the energy price scenarios with high mean and low variance.

EGR	System	TC scenario	TAC [Million euro]	TAC reduction [%]	NG to system [GWh]	Power grid to system [GWh]	System to power grid [GWh]
1.6	Reference	–	12.0		202.1	0	39.5
	New	HighHP-LowRest	10.7	11.3	109.3	8.5	2.9
	New	LowHP-HighRest	10.2	15.4	107.5	10.1	3.5
1	Reference	–	19.4		195.0	0	34.1
	New	HighHP-LowRest	14.6	24.6	104.6	11.4	2.5
	New	LowHP-HighRest	14.1	27.2	104.6	12.0	3.5

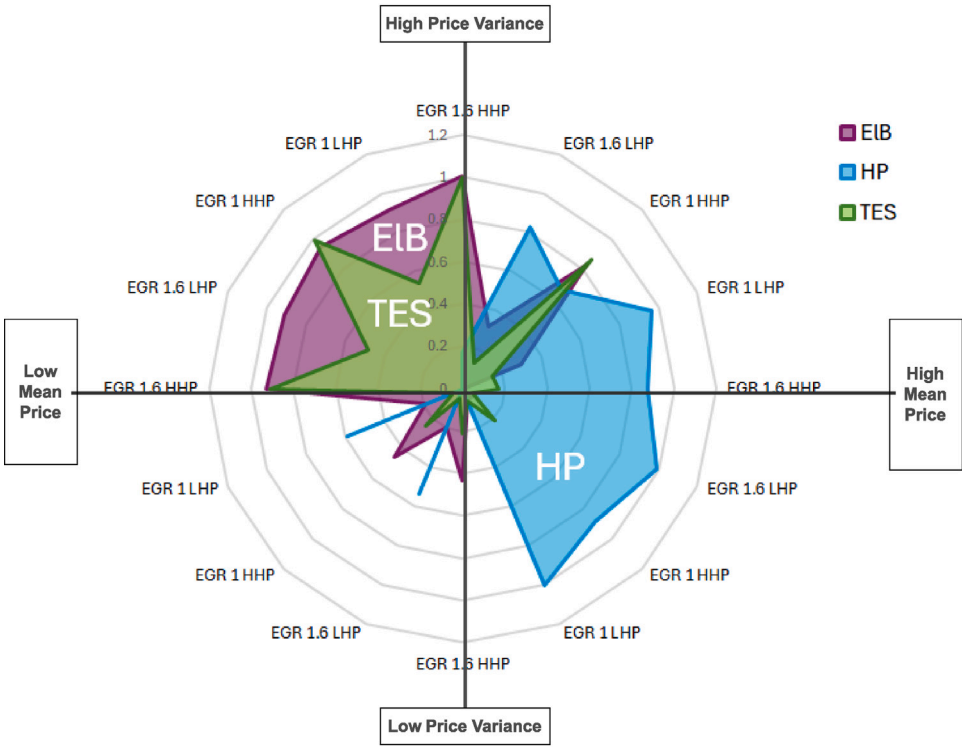

Fig. 9. Overview of normalised installed capacities across all scenarios. The right half of the diagram shows the installed capacities in energy price scenarios with a high mean price, and the upper half for scenarios with a high price variance.

scenarios with high mean prices on the left side of Fig. 9, and large ElBs are predominantly installed in the case of low and volatile energy prices, depicted on the right side of the figure. The large ElBs are combined with large TES, sized according to equipment cost. The highest HPs are installed when prices are, on average, high and show small fluctuations ('High mean low variance' scenarios). In these scenarios, neither the relative HP cost nor the electricity-to-gas price ratio leads to significant changes in the HP capacity. The large HPs in these scenarios are economically viable despite lower load factors because higher mean electricity prices lead to overall higher operational costs, which in turn leave more room for additional investment that enables operational cost savings.

Fig. 9 shows that Elb and HP capacities are combined in the energy price scenarios with a low mean and low variance (LMLV), and with a high mean and a high variance (HMHV). In the LMLV scenarios, HP and ElB capacities are low, as energy prices are too low to justify the investment in HPs and too stable for large ElBs. In the HMHV scenarios, the large positive and negative price peaks lead to a large (26 MW) ElB capacity alongside a 6 MW HP and a 97 MWh TES when the equipment cost of the HP is high ('HMHV HighHP-LowRest'). The HP load factor ranges from 78 to 92%, which means that the HP operates as base load technology next to the CHP and confirms that high mean energy prices are required for the installation of HPs.

When an HP is installed, its size is affected by the EGR when HP capacities are below 5 MW, as seen in Table 10. Higher capacities of the HP are installed when the mean gas price is equal to the electricity price because switching from gas to electricity use leads to higher cost savings than in the scenarios with a lower gas price. The observed threshold of 5 MW can be explained by looking at Fig. 10. The curve declines sharply around 12 MW. Since the CHP has to operate at minimal load at all times, the steady heat output of the CHP of around 6.5 MW reduces the heat that is required during around 7000 h per year to 5.5 MW. HPs that operate above 5.5 MW, therefore, operate with a lower load factor and are only economically viable under HP-favourable conditions, i.e. high mean electricity prices. HPs that operate under those conditions are less sensitive to the EGR.

4. Limitations of the study

Though the results provide valuable insights for electrifying utility systems for the energy-intensive industry with fluctuating energy demand, the chosen method, assumptions, and scenarios have limitations. This section addresses them, offering important considerations for interpreting the results of this study.

The selected energy price scenarios are based on the assumption that companies pay for all their CO_2 emissions. Allowing free allocation

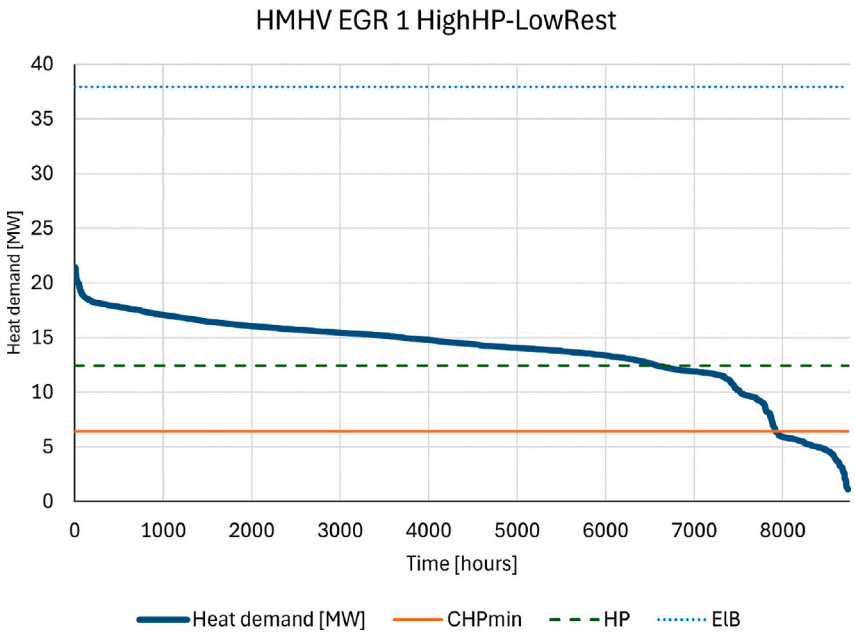

Fig. 10. Heat demand duration curve with the minimal heat output by the CHP and the added capacities by the HP and ElB in the HMHV EGR 1 HighHP-LowRest scenario.

of CO_2 permits would increase the EGR and likely limit the electrification technologies' economic viability. Additional price scenarios could be added to the analysis to explore "tipping points" for increasing levels of electrification.

Including the cost of energy transport in the model, such as network cost and peak tariffs, is also likely to affect the capacities and may reduce the share of electrification seen in the results. The authors expect that the effect would be more significant for the ElB capacity due to its less efficient use of electricity compared to an HP. Peak tariffs would likely lead to decreased ElB and TES capacities because they disincentivise the consumption of large amounts of power. However, transport costs would not need to be added to the consumption of power generated by the CHP. Therefore, it would not affect the power exchange between the CHP and the PtH technologies, which is high in the systems presented. Hence, (partial) electrification of utility systems is likely still cost-optimal if grid use costs were included in the model.

The explored energy price scenarios do not account for energy price uncertainty since the system has perfect foresight. Accounting for operational difficulties any system encounters in the real world, where prices might deviate from the forecast, would result in capacities different from those presented, especially those of the storage units. Stochastic programming could be used to explore this aspect in future studies.

The main objective of the model is to minimise the total annual cost of the utility system. While this performance indicator provides valuable insights, other aspects, such as payback time and environmental impact, have not been considered, despite their importance to industry [39]. Including these indicators will likely result in other optimal solutions. The CO_2 emissions related to grid electricity (scope 2 emissions) are currently not considered in the model as they are case-specific and subject to change due to the ongoing decarbonisation of the national power generation. The model could be extended to include multiple objectives to explore the trade-offs between CO_2 emission reduction and TAC. This would likely result in higher PtH capacities, especially HP capacity, because of their conversion efficiency.

The sizing of the HP, ElB and other technologies also depends on the selected discount rate of 10%, and the absence of eventual retrofitting costs for the CHP in the model. A lower discount rate would incentivise investments and lead to larger installed capacities. The need to invest in the CHP due to required maintenance or retrofitting would likely have a similar effect. Larger PtH and storage capacities were also observed in model runs without the constraint limiting the CHP's operation to a minimum of 30% of its capacity. These results and a brief discussion are included in Appendix C. They indicate that more flexible CHPs would likely supply less energy to the process lead to higher levels of electrification in the utility system.

In this study, a CHP exists before electrifying the utility system. Since the results show that PtH and storage technologies use power generated by the CHP, the results would change if the CHP did not exist.

The model was used to study the optimal electrification of a utility system for a paper mill with a grid connection capacity of 30 MW, which exists because of the plant's previous role as energy supplier. The size of the grid connection affects the sizing of the PtH technologies. The results show that the ElB is sized to this capacity when energy prices are highly volatile. Hence, a smaller connection capacity would result in a smaller ElB. As a consequence, the TES would be charged less and potentially scaled down. The size of the grid connection is likely to also affect the sizing of the HP, but only in cases when the HP's size exceeds that of the grid connection.

The variable operation of the utility system result in part-load operation of the PtH technologies. While this is not expected to affect the ElB, it would lead to a suboptimal efficiency of the HP. However, a change in the HP's efficiency in part load operation is neglected in the model to decrease its complexity. Accounting for it could lead to changes in HP capacity. Either the capacity would decrease while operation at full capacity would be increased, or the capacities would remain, but the share of heat generation of the HP would increase by reducing the use of any of the other technologies.

Finally, the TES in this study is modelled based on a latent heat storage unit with isothermal operation. This technology was selected based on the isothermal temperature supply by the HP for effective implementation [40]. When multiple TES systems were to be considered, the high-temperature potential of direct electrification could be combined with sensible heat storage that comes at a lower cost than latent heat storage [27]. The option for cheaper TES capacity might lead to higher ElB capacities.

5. Conclusions and recommendations for future work

This study presented an analysis of the influence of energy prices on the electrification of industrial utility systems for processes with highly variable energy demand. To this end, energy price profiles with differing average prices and variances and technology cost scenarios were explored. The analyses were carried out for a paper mill in the Netherlands with an existing utility system comprising a CHP and a connection to the national power grid of 30 MW.

The results show that under the assumed technical and economic conditions (presented in Tables 3–5), electrification reduces the total annual cost by between 11 and 52 per cent. The model added heat pumps and/or electric boilers and thermal energy storage to the existing utility system; batteries and hydrogen technologies were not selected. A sensitivity analysis, presented and briefly discussed in Appendix B, shows that the cost for the electrolyser capacity has to decrease by between one and more than three orders of magnitude (depending on the energy price scenario) to become part of the cost-optimal technology portfolio. The difference between the scenarios is likely due to the number of hours with negative electricity prices, which allow the system to generate revenues because of the losses in hydrogen production. The fact that hydrogen is not picked up by the model can thus be explained by the high upfront cost. Therefore, we conclude that for the explored energy price and technology cost scenarios, hydrogen as an energy carrier is not required for cost-optimal electrification, as long as temperature requirements do not exceed what electric boilers and heat pumps can deliver. Using hydrogen might become more interesting when energy prices are high for extended periods of time, and the required storage capacity would become larger, as hydrogen storage costs are lower than the cost for alternative means of energy storage.

The heat supplied by the CHP is reduced to the minimum possible amount in most scenarios and replaced by power-to-heat and storage technologies. By using a large share of the power generated by the CHP to run the power-to-heat technologies, the amount of power sold to the grid is reduced compared to the reference case without power-to-heat and storage technologies.

Heat pumps are sized based on the process's heat demand duration curve, the minimal load of the CHP and the mean energy price. High and stable energy prices lead to the largest installed heat pump capacities. Lower energy prices limit the profitability of the investment-intensive heat pump and result in smaller capacities. The impact of the relative technology cost of heat pumps on their size increases with the variance of energy prices because the heat pump competes with the electric boiler and thermal energy storage, which have a lower cost and are, therefore, the cheaper peak technology.

The size of the electric boiler is mainly defined by the variance of electricity prices and is limited by the size of the grid connection and the thermal energy storage capacity. The operation of all components is a function of the electricity-to-gas-price ratio and the absolute electricity price.

It is recommended to further study utility system electrification. The presented model can serve as a basis for future research, which should explore valuing flexibility by (a) assessing different energy markets (e.g., imbalance markets) and (b) providing grid services. Moreover, including uncertainty in the analysis would add further understanding of optimal electrification strategies for industries with fluctuating energy demand.

List of abbreviations

Bat	Battery
CaPex	Capital expenditure
CHP	Combined heat and power plant
CO_2	Carbon Dioxide
COP	Coefficient of performance
EGR	Electricity-to-gas price ratio
ElB	Electric boiler
EU ETS	EU Emissions Trading System
GB	Gas boiler
GHG	Greenhouse gases
GT	Gas turbine
H2	Hydrogen
H2B	Hydrogen boiler
H2E	Electrolyser
H2S	Hydrogen storage tank
HMHV	High Mean High Variance
HMLV	High Mean Low Variance
HP	Heat pump
HRSG	Heat recovery steam generator
LMHV	Low Mean High Variance
LMLV	Low Mean Low Variance
NG	Natural gas
OpEx	Operating expense
PtH	Power-to-heat
TAC	Total Annual Cost
TC	Technology Cost
TES	Thermal energy storage
TTF	Title Transfer Facility

Nomenclature

Nomenclature of parameters and variables

Symbol	Explanation	Unit
Time-dependent variables (per time step)		
$H_{\mathrm{CHP,out}}(t)$	Heat output from the combined heat and power unit	MW
$H_{\mathrm{HP,out}}(t)$	Heat output from the heat pump	MW
$H_{\mathrm{HP,out}}(t)$	Heat produced by the combined heat and power unit	MW
$NG_{\mathrm{in}}(t)$	Quantity of natural gas consumed	MW
$NG_{\mathrm{GT,in}}(t)$	Natural gas input to the gas turbine	MW
$NG_{\mathrm{GB,in}}(t)$	Natural gas input to the gas boiler	MW
$P_{\mathrm{gr,i}}(t)$	Power from the power grid to technology i	MW
$P_{\mathrm{i,gr}}(t)$	Power from technology i to the power grid	MW
$P_{\mathrm{gr,process}}(t)$	Power from the power grid to the process	MW
$P_{\mathrm{GT,gr}}(t)$	Power from the gas turbine to the power grid	MW
$P_{\mathrm{GT,process}}(t)$	Power from the gas turbine to the process	MW
$P_{\mathrm{GT,bat}}(t)$	Power from the gas turbine to the battery	MW
$P_{\mathrm{HP,in}}(t)$	Power flow to the heat pump	MW
Sizing variables		
s_{i}	Size of technology i	MW or MWh
Time-dependent parameters		
$p_{\mathrm{el,grid}}(t)$	Electricity price at time t	Eur/MWh

$p_{NG}(t)$	Natural gas price at time t	Eur/MWh
$H_{dem}(t)$	Heat demand of the process at time t	MW
$P_{dem}(t)$	Power demand of the process at time t	MW
Constants		
AF_i	Annualisation factor of technology i	–
c_i	Capital cost of component i	Eur/unit
COP_{ideal}	Carnot Coefficient of Performance	–
$H_{dem,max}$	Maximal heat demand	MW
Inf_i	Installation or Lang factor of technology i	–
LT_i	Lifetime of component i	years
r	Discount rate	%
T_{sink}	Temperature of the heat sink of the heat pump	K
T_{source}	Temperature of the heat source of the heat pump	K
Δt	Time step duration	h
η	Efficiency	–
$\eta_{i,th}$	Thermal efficiency of technology i	–
$\eta_{i,el}$	Electric efficiency of technology i	–

CRediT authorship contribution statement

Svenja Bielefeld: Writing – review & editing, Writing – original draft, Visualization, Validation, Software, Methodology, Formal analysis, Data curation, Conceptualization. **Brendon de Raad:** Writing – review & editing, Writing – original draft, Visualization, Validation, Software, Methodology, Formal analysis, Data curation, Conceptualization. **Lydia Stougie:** Writing – review & editing, Supervision, Methodology, Conceptualization. **Miloš Cvetković:** Writing – review & editing, Supervision, Methodology, Conceptualization. **Marit van Lieshout:** Writing – review & editing, Supervision, Methodology, Funding acquisition, Conceptualization. **Andrea Ramírez:** Writing – review & editing, Supervision, Methodology, Funding acquisition, Conceptualization.

Declaration of competing interest

The authors declare that they have no known competing financial interests or personal relationships that could have appeared to influence the work reported in this paper.

Acknowledgements

This work is part of the RELEASE project, and partially funded by the Dutch Research Council (NWO) [project number 17621]. This research publication is also partly funded by the Dutch Government Office for Enterprising (RVO) within the framework of the Mission-driven Research, Development, and Innovation funds (MOOI) under the project title: "THIO — The Heat is On" under the lead of the Dutch Institute for Sustainable Process industry (ISPT). The icons used in Figs. 1 and 2 are obtained from https://thenounproject.com/. The Sankey diagrams are made with SankeyMATIC (https://sankeymatic.com/). The authors used Grammarly and Microsoft Copilot to improve the writing and formatting of the manuscript. The authors reviewed the content and take full responsibility for it.

Appendix A. Energy price and technology cost scenarios

To study the impact of changes in the energy and technology cost on the results of the model sixteen scenarios were formulated. Figs. A.11 to A.14 show the energy price profiles in these scenarios, presented in 2.5.1. Fig. A.11 depicts the energy prices in the LMLV scenario. It clearly shows the difference in volatility between the electricity prices (EP) and the gas prices (GP). Moreover, it shows how the two gas prices differ in the EGR scenarios, with the 'EGR 1' being the scenario with the highest average price. The ratio between the GP in EGR 1 and the GP in EGR 1.6 is the same in Figs. A.12 to A.14. Fig. A.15 shows how the different energy price scenarios are combined with the technology cost scenarios.

Appendix B. Electrolyser technology cost sensitivity analysis

To enhance the understanding of why hydrogen is not selected by the model in any of the results presented in Section 3, a sensitivity analysis of the electrolyser cost was carried out. The two energy cost scenarios with the highest deviation in terms of electricity prices were selected for the analysis: 'Low Mean High Variance' with EGR 1.6 and 'High Mean High Variance' with EGR 1. In both cases, the TC scenario unfavourable for HPs and favourable for alternative technologies, such as the electrolyser, was chosen. The technology cost of the electrolyser was decreased until hydrogen was picked up by the model. The cost was decreased by one order of magnitude at the time until hydrogen started appearing in the technology portfolio. Then, the price was increased again. For the 'Low Mean High Variance' scenario, the step size was increased by halving the difference between the steps until the tipping point was found to be at 9% of the original technology cost. For the 'High Mean High Variance' scenario, the cost first had to be decreased to 0.1% of the original cost (76 euro/MW). Subsequently, the cost was doubled, and then decreased by steps of 50 euro/kW. The results of the sensitivity analysis for which hydrogen is and is not part of the cost-optimal technology portfolio are presented in Tables B.14 and B.15. For the 'Low Mean High Variance' energy price scenario, with relatively many negative electricity price hours, the cost has to decrease more than one order of magnitude, from 760 euro/kW to 68.4 euro/kW. For the 'High Mean High Variance' scenario, the cost has to be as low as 0.2 euro/kW.

Appendix C. Results without the minimal load constraint of the CHP

Tables C.16, C.17, C.18, and C.19 show the technology portfolio of the cost-optimal utility system if the CHP operation is not constrained and can shut down completely. Omitting this constraint and accepting it, though not accounting for the increase in maintenance cost, results in the following changes to the sizing and operation of the PtH technologies. For low and stable electricity prices, more PtH technologies are installed (see Table C.16). The size of the HP increases with the previous minimal capacity of the CHP. The combined capacity of TES and ElB increases by a factor of 2. When price fluctuations increase, the change in capacities is limited as the size of ElB and the TES are already limited by the grid connection capacity of the system (see C.17). Nevertheless, less natural gas is consumed overall. When the mean energy price increases, the size of the ElB reduces, the capacity of the TES remains the same, and the size of the HP increases compared to the scenario with the CHP constraint (see C.18). Reducing price fluctuations whilst maintaining the high mean energy price results in the same increase in HP capacity, whilst the capacities of the TES and ElB remain relatively unchanged (see C.19). Though the total natural gas consumption is reduced in all scenarios when the CHP is allowed to shut down completely, complete electrification is only cost-optimal in the scenario with high mean prices, low price fluctuations and a low electricity-to-gas-price ratio.

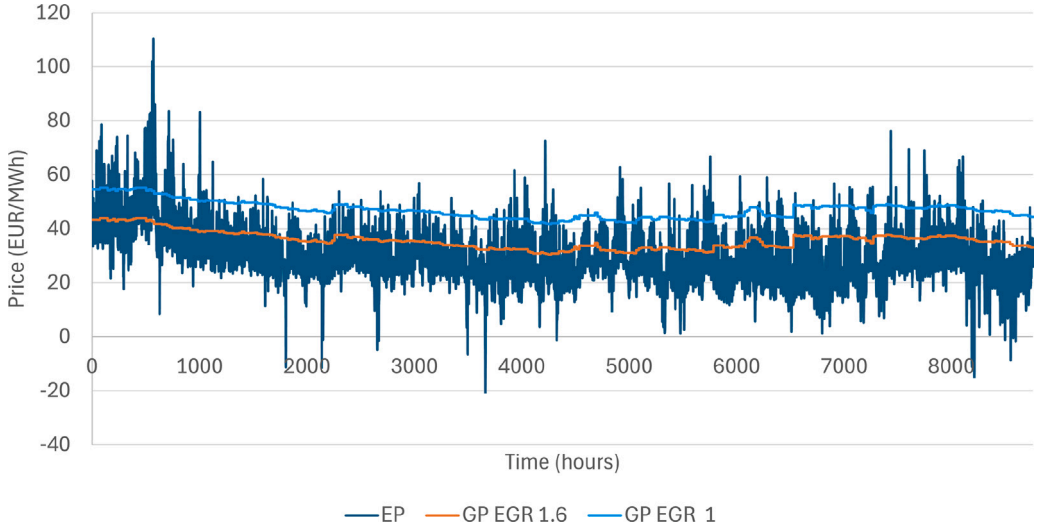

Fig. A.11. The electricity (EP) and gas (GP) prices for the electricity-to-gas ratio (EGR) of 1.6 and 1 for the 'Low Mean Low Variance' scenario.

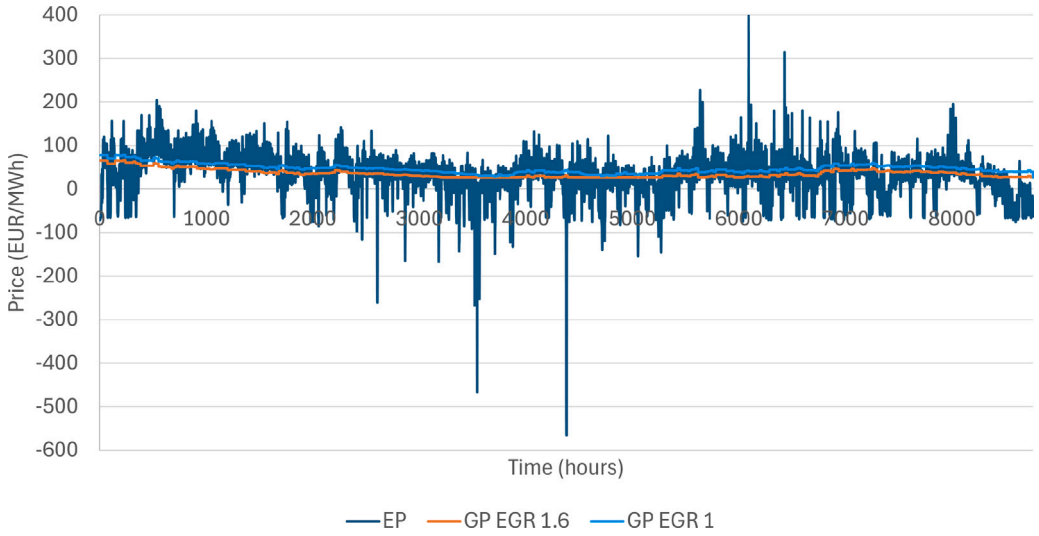

Fig. A.12. The electricity (EP) and gas (GP) prices for the electricity-to-gas ratio (EGR) of 1.6 and 1 for the 'Low Mean High Variance' scenario.

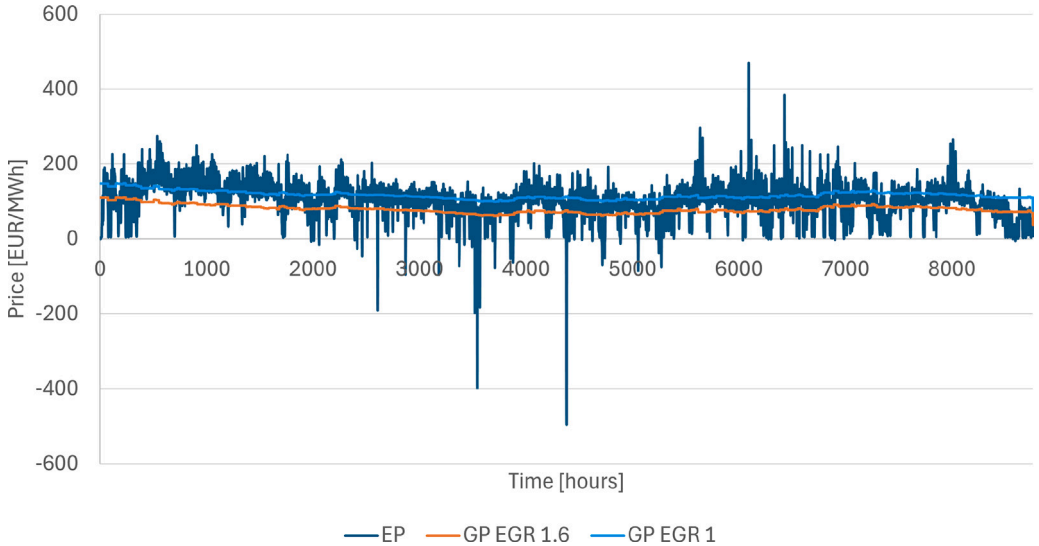

Fig. A.13. The electricity (EP) and gas (GP) prices for the electricity-to-gas ratio (EGR) of 1.6 and 1 for the 'High Mean High Variance' scenario.

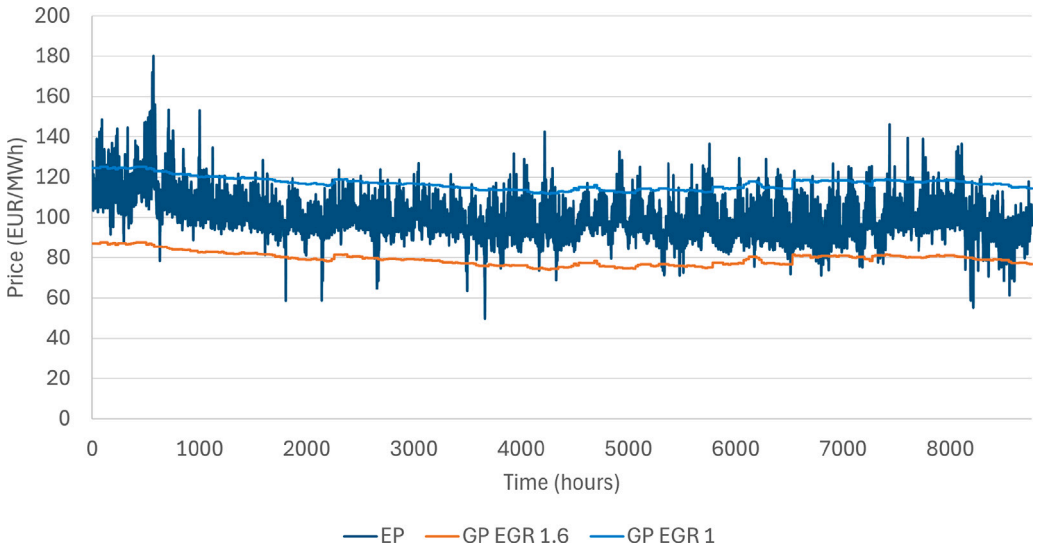

Fig. A.14. The electricity (EP) and gas (GP) prices for the electricity-to-gas ratio (EGR) of 1.6 and 1 for the 'High Mean Low Variance' scenario.

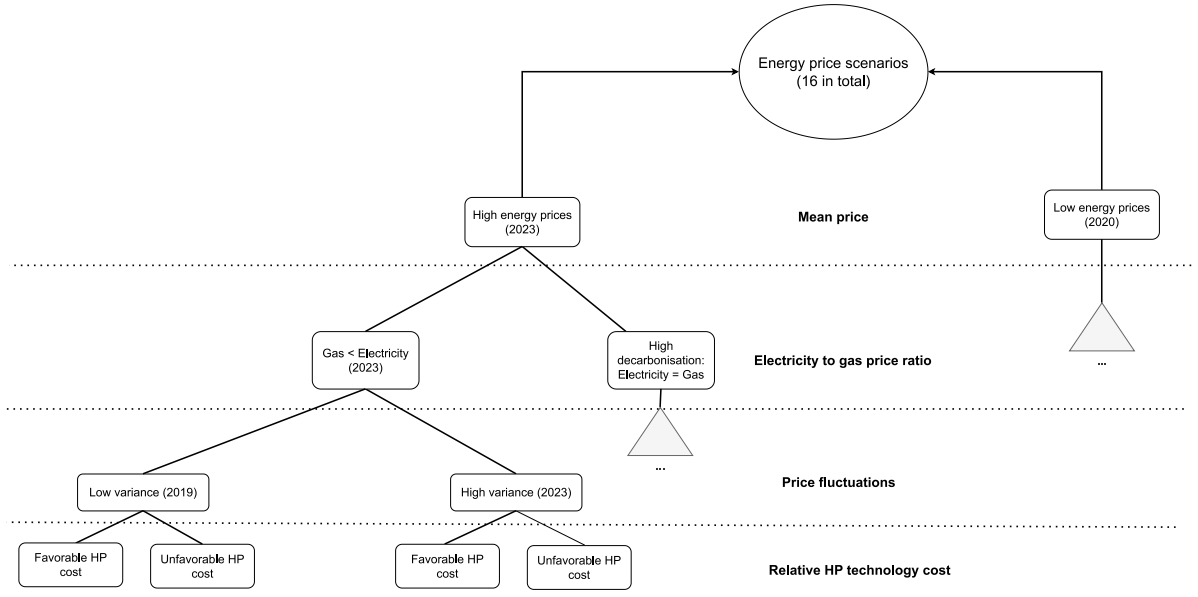

Fig. A.15. Scenario tree considering the mean energy price, the electricity-to-gas price ratio, the energy price fluctuations and the technology cost.

Table B.14
Installed PtH and storage capacities in the energy price scenario with low mean and high variance for different electrolyser technology costs.

TC_{H2E} [euro/MW]	EGR	TC cost scenario	ElB [MW_{th}]	TES [MWh]	HP [MW_{th}]	H2E [MW]	H2B [MW]	H2S [MWh]
68400	1.6	'HighHP-LowRest'	28.4	100.5	0	0.3	0.2	0
76000	1.6	'HighHP-LowRest'	29	103	0	0	0	0

Table B.15
Installed PtH and storage capacities in the energy price scenario with high mean and high variance for different electrolyser technology costs.

TC_{H2E} [euro/MW]	EGR	TC cost scenario	ElB [MW_{th}]	TES [MWh]	HP [MW_{th}]	H2E [MW]	H2B [MW]	H2S [MWh]
200	1	'HighHP-LowRest'	22.3	85.7	6.1	7.6	0.4	7.5
250	1	'HighHP-LowRest'	26.5	92.2	6.1	0	0	0

Table C.16
Installed PtH and storage capacities in the energy price scenarios with low mean and variance.

EGR	TC cost scenario	ElB [MW_{th}]	TES [MWh]	HP [MW_{th}]
1.6	HighHP-LowRest	24	42	0
	LowHP-HighRest	6	5	11
1	HighHP-LowRest	25	49	0
	LowHP-HighRest	6	6	12

Table C.17
Installed PtH and storage capacities in the energy price scenarios with low mean and high variance.

EGR	TC cost scenario	ElB [MW_{th}]	TES [MWh]	HP [MW_{th}]
1.6	HighHP-LowRest	29	103	0
	LowHP-HighRest	28	62	0
1	HighHP-LowRest	29	113	0
	LowHP-HighRest	28	68	0

Table C.18
Installed PtH and storage capacities in the energy price scenarios with high mean and high variance.

EGR	TC cost scenario	ElB [MW_{th}]	TES [MWh]	HP [MW_{th}]
1.6	HighHP-LowRest	24	94	8
	LowHP-HighRest	7	15	14
1	HighHP-LowRest	22	96	13
	LowHP-HighRest	6	18	15

Table C.19
Installed PtH and storage capacities in the energy price scenarios with high mean and low variance.

EGR	TC cost scenario	ElB [MW_{th}]	TES [MWh]	HP [MW_{th}]
1.6	HighHP-LowRest	0	19	14
	LowHP-HighRest	0	6	15
1	HighHP-LowRest	2	22	14
	LowHP-HighRest	2	6	16

Appendix D. Model formulation

D.1. Nomenclature of parameters and variables

Symbol	Explanation	Unit
Time-dependent variables		
$P_{\mathrm{gr,ElB}}(t)$	Grid power to the electric boiler	MW
$P_{\mathrm{gr,process}}(t)$	Grid power to the process	MW
$P_{\mathrm{gr,bat}}(t)$	Grid power to the battery	MW
$P_{\mathrm{gr,H2E}}(t)$	Grid power to the electrolyser	MW
$P_{\mathrm{gr,HP}}(t)$	Grid power to the heat pump	MW
$P_{\mathrm{GT,gr}}(t)$	Power from gas turbine to grid	MW
$P_{\mathrm{GT,process}}(t)$	Power from gas turbine to process	MW
$P_{\mathrm{GT,bat}}(t)$	Power from gas turbine to battery	MW
$P_{\mathrm{GT,ElB}}(t)$	Power from gas turbine to electric boiler	MW
$P_{\mathrm{GT,HP}}(t)$	Power from gas turbine to heat pump	MW
$P_{\mathrm{GT,H2E}}(t)$	Power from gas turbine to electrolyser	MW
$P_{\mathrm{GT,excess}}(t)$	Excess power from gas turbine	MW
$P_{\mathrm{bat,process}}(t)$	Power from battery to the process	MW
$P_{\mathrm{bat,gr}}(t)$	Power from battery to grid	MW
$P_{\mathrm{bat,ElB}}(t)$	Power from battery to electric boiler	MW
$P_{\mathrm{bat,H2E}}(t)$	Power from battery to electrolyser	MW
$P_{\mathrm{bat,HP}}(t)$	Power from battery to heat pump	MW
$H_{\mathrm{ElB,process}}(t)$	Heat generated by electric boiler for the process	MW
$H_{\mathrm{CHP,process}}(t)$	Heat generated by the CHP for the process	MW
$H_{\mathrm{HP,process}}(t)$	Heat generated by the heat pump for the process	MW
$H_{\mathrm{TES,process}}(t)$	Heat from thermal energy storage to the process	MW
$H_{\mathrm{H2B,process}}(t)$	Heat from the hydrogen boiler to the process	MW
$H_{\mathrm{CHP,TES}}(t)$	Heat from CHP to thermal energy storage	MW
$H_{\mathrm{CHP,excess}}(t)$	Excess heat from CHP	MW
$H_{\mathrm{ElB,TES}}(t)$	Heat from electric boiler to thermal energy storage	MW
$H_{\mathrm{HP,TES}}(t)$	Heat from heat pump to thermal energy storage	MW
$NG_{\mathrm{GT,in}}(t)$	Natural gas input to the gas turbine	MW
$NG_{\mathrm{GB,in}}(t)$	Natural gas input to the gas boiler	MW
$H_{2,\mathrm{H2E,H2B}}(t)$	Hydrogen from electrolyser to the boiler	MW
$H_{2,\mathrm{H2E,H2S}}(t)$	Hydrogen from electrolyser to storage	MW
$H_{2,\mathrm{H2S,H2B}}(t)$	Hydrogen from storage to the boiler	MW
$SOE_{\mathrm{bat}}(t)$	State of energy of the battery	MWh
$SOE_{\mathrm{TES}}(t)$	State of energy in the thermal energy storage	MWh
$SOE_{\mathrm{H2S}}(t)$	State of energy in hydrogen storage	kg
$b_1(t)$	Binary variable for battery charging	Binary (0/1)
$b_2(t)$	Binary variable for thermal energy storage charging	Binary (0/1)
$b_3(t)$	Binary variable for hydrogen storage tank	Binary (0/1)
$b_4(t)$	Binary variable for grid connection	Binary (0/1)
Sizing variables		
s_{ElB}	Electric boiler size	MW_{th}
s_{HP}	Heat pump size	MW_{th}
s_{H2E}	Electrolyser size	MW_{el}

s_{H2B}	Hydrogen boiler size	MW_{th}
s_{TES}	Thermal energy storage size	MWh
s_{H2S}	Hydrogen storage size	MWh
s_{bat}	Battery size	MWh

Time-dependent parameters

$\mathrm{p}_{\mathrm{el,grid}}(t)$	Electricity price at time t	Eur/MWh
$\mathrm{p}_{\mathrm{NG,use}}(t)$	Price for using natural gas price at time t[a]	Eur/MWh
$H_{\mathrm{dem}}(t)$	Heat demand of the process at time t	MW
$P_{\mathrm{dem}}(t)$	Power demand of the process at time t	MW

Constants

s_{GT}	Gas turbine size	MW
s_{GB}	Gas boiler size	MW
r_{disc}	Discount rate	%
Δt	Time step duration	h
$\eta_{\mathrm{GT,el}}$	Gas turbine electric efficiency	–
$\eta_{\mathrm{GT,th}}$	Gas turbine thermal efficiency	–
η_{GB}	Gas boiler efficiency	–
η_{ElB}	Electric boiler efficiency	–
$\mathrm{COP}_{\mathrm{HP,Carnot}}$	Heat pump ideal coefficient of performance	–
η_{HP}	Heat pump efficiency	–
η_{H2E}	Hydrogen electrolyser efficiency	–
η_{H2B}	Hydrogen boiler efficiency	–
η_{bat}	Battery charge and discharge efficiency	–
η_{TES}	Thermal energy storage efficiency	–
η_{H2S}	Hydrogen storage efficiency	–
$\mathrm{MinLoadFactor}_{\mathrm{GT}}$	Minimum load factor for gas turbine	% of capacity
$\mathrm{crate}_{\mathrm{bat}}$	Charge/discharge rate of battery	MW/MWh
$\mathrm{crate}_{\mathrm{TES}}$	Charge/discharge rate of thermal energy storage	MW/MWh
$\mathrm{cap}_{\mathrm{gr}}$	Grid connection capacity	MW
c_i	Capital cost of component i	Eur/unit
$\mathrm{Inf_i}$	Installation or Lang factor of technology i	–
LT_i	Lifetime of component i	years

[a] Includes price for CO_2 emissions.

D.2. Mathematical formulations of the reference model

The following equations are used to calculate the performance of the reference model.

Objective function.

$$min \sum_{t=0}^{t=16000} \mathrm{OpEx}(t), \tag{D.1}$$

where

$$\mathrm{OpEx}(t) = \mathrm{p}_{\mathrm{el,grid}}(t) \cdot \Delta t \cdot \left(P_{\mathrm{gr,\ process}}(t) - P_{\mathrm{GT,\ gr}}(t) \right) + \left(NG_{\mathrm{GT,in}}(t) + NG_{\mathrm{GB,in}}(t) \right) \cdot \Delta t \cdot \mathrm{p}_{\mathrm{NG,use}}(t)$$

Energy balance equality constraints. Heat balance:

$$H_{\mathrm{dem}} = H_{\mathrm{CHP,process}}(t), \tag{D.2}$$

Power balance:

$$P_{\mathrm{dem}} = P_{\mathrm{gr,process}}(t) + P_{\mathrm{GT,process}}(t) \tag{D.3}$$

CHP constraints. Power generation constraint:

$$NG_{\mathrm{GT,in}}(t) \cdot \eta_{\mathrm{GT,el}} = P_{\mathrm{GT,excess}}(t) + P_{\mathrm{GT,process}}(t) + P_{\mathrm{GT,gr}}(t) \tag{D.4}$$

Heat generation constraint:

$$\left(NG_{\mathrm{GT,in}}(t) \cdot \eta_{\mathrm{GT,th}} + NG_{\mathrm{GB,in}}(t) \right) \cdot \eta_{\mathrm{GB}} = H_{\mathrm{CHP,process}}(t) + H_{\mathrm{CHP,excess}}(t) \tag{D.5}$$

Maximum natural gas consumption constraints:

$$NG_{\mathrm{GT,in}}(t) \leq \frac{s_{\mathrm{GT}}}{\eta_{\mathrm{GT,th}}} \tag{D.6}$$

and

$$NG_{\mathrm{GB,in}}(t) \leq \frac{s_{\mathrm{GB}}}{\eta_{\mathrm{GB,th}}} \tag{D.7}$$

Minimal load constraint:

$$NG_{\mathrm{GT,in}}(t) \geq \frac{s_{\mathrm{GT}}}{\eta_{\mathrm{GT,th}}} \cdot \mathrm{MinLoadFactor}_{\mathrm{GT}} \tag{D.8}$$

Grid connection capacity. Maximum inflow constraint:

$$\mathrm{cap}_{\mathrm{gr}} \cdot b_3(t) \geq P_{\mathrm{gr,process}}(t) \tag{D.9}$$

Maximum outflow constraint:

$$P_{\mathrm{GT,gr}}(t) \leq \mathrm{cap}_{\mathrm{gr}} \cdot (1 - b_3(t)) \tag{D.10}$$

D.3. Mathematical formulations of the model for the electrification of the utility system

The following equations represent the mathematical formulation of the model for the electrification of the utility system.

Objective function.

$$min \sum_{t=0}^{t=16000} \mathrm{OpEx}(t) + \mathrm{CaPex}, \tag{D.11}$$

where

$$\mathrm{OpEx}(t) = \mathrm{p}_{\mathrm{el,grid}}(t) \cdot \Delta t \cdot \Big(P_{\mathrm{gr,\ ElB}}(t) + P_{\mathrm{gr,\ process}}(t) + P_{\mathrm{gr,\ bat}}(t) + P_{\mathrm{gr,\ H2E}}(t) + P_{\mathrm{gr,\ HP}}(t) - \left(P_{\mathrm{GT,\ gr}}(t) + P_{\mathrm{bat,\ gr}}(t) \right) \Big) + \left(NG_{\mathrm{GT,in}}(t) + NG_{\mathrm{GB,in}}(t) \right) \cdot \Delta t \cdot \mathrm{p}_{\mathrm{NG,use}}(t) \tag{D.12}$$

and

$$\mathrm{CaPex} = \sum_{i \in \{\mathrm{HP,bat,ElB,TES,H2E,H2B,H2S}\}} \frac{s_i \cdot c_i \cdot \mathrm{Inf}_i \cdot r_{\mathrm{disc}}}{1 - (1 + r_{\mathrm{disc}})^{-\mathrm{LT}_i}} \tag{D.13}$$

Energy balance equality constraints. Heat balance:

$$H_{\mathrm{dem}}(t) = H_{\mathrm{ElB,CP}}(t) + H_{\mathrm{CHP,CP}}(t) + H_{\mathrm{TES,CP}}(t) + H_{\mathrm{H2B,CP}}(t) + H_{\mathrm{HP,CP}}(t) \tag{D.14}$$

Power balance:

$$P_{\mathrm{dem}}(t) = P_{\mathrm{gr,process}}(t) + P_{\mathrm{GT,process}}(t) + P_{\mathrm{bat,process}}(t) \tag{D.15}$$

CHP constraints. Power generation constraint:

$$NG_{\mathrm{GT,in}}(t)\cdot\eta_{\mathrm{GT,el}} = P_{\mathrm{GT,excess}}(t) + P_{\mathrm{GT,bat}}(t) + P_{\mathrm{GT,ElB}}(t) + P_{\mathrm{GT,H2E}}(t) + P_{\mathrm{GT,HP}}(t) + P_{\mathrm{GT,process}}(t) + P_{\mathrm{GT,gr}}(t) \quad \text{(D.16)}$$

Heat generation constraint:

$$\left(NG_{\mathrm{GT,in}}(t)\cdot\eta_{\mathrm{GT,th}} + NG_{\mathrm{GB,in}}(t)\right)\cdot\eta_{\mathrm{GB}} = H_{\mathrm{CHP,process}}(t) + H_{\mathrm{CHP,TES}}(t) + H_{\mathrm{CHP,excess}}(t) \quad \text{(D.17)}$$

Maximum natural gas consumption constraints:

$$NG_{\mathrm{GT,in}}(t) \le \frac{s_{\mathrm{GT}}}{\eta_{\mathrm{GT,th}}} \quad \text{(D.18)}$$

and

$$NG_{\mathrm{GB,in}}(t) \le \frac{s_{\mathrm{GB}}}{\eta_{\mathrm{GB,th}}} \quad \text{(D.19)}$$

Minimal load constraint:

$$NG_{\mathrm{GT,in}}(t) \ge \frac{s_{\mathrm{GT}}}{\eta_{\mathrm{GT,th}}}\cdot \mathrm{MinLoadFactor}_{\mathrm{GT}} \quad \text{(D.20)}$$

Electric boiler. Heat generation constraint:

$$H_{\mathrm{ElB,process}}(t) + H_{\mathrm{ElB,TES}}(t) = \left(P_{\mathrm{gr,ElB}}(t) + P_{\mathrm{bat,ElB}}(t) + P_{\mathrm{GT,ElB}}(t)\right)\cdot\eta_{\mathrm{ElB}} \quad \text{(D.21)}$$

Sizing constraint:

$$H_{\mathrm{ElB,process}}(t) + H_{\mathrm{ElB,TES}}(t) \le s_{\mathrm{ElB}} \quad \text{(D.22)}$$

Heat pump. Heat generation constraint:

$$H_{\mathrm{HP,process}}(t) + H_{\mathrm{HP,TES}}(t) = \left(P_{\mathrm{gr,HP}}(t) + P_{\mathrm{bat,HP}}(t) + P_{\mathrm{GT,HP}}(t)\right)\cdot \mathrm{COP}_{\mathrm{Carnot,HP}}\cdot\eta_{\mathrm{HP}} \quad \text{(D.23)}$$

Sizing constraint:

$$H_{\mathrm{HP,process}}(t) + H_{\mathrm{HP,TES}}(t) \le s_{\mathrm{HP}} \quad \text{(D.24)}$$

Water electrolyser. Hydrogen production constraint:

$$\left(P_{\mathrm{gr,H2E}}(t) + P_{\mathrm{bat,H2E}}(t)\right)\cdot\eta_{\mathrm{H2E}} = H_{\mathrm{2,H2E,H2B}}(t) + H_{\mathrm{2,H2E,H2S}}(t) \quad \text{(D.25)}$$

Sizing constraint:

$$P_{\mathrm{gr,H2E}}(t) + P_{\mathrm{bat,H2E}}(t) \le s_{\mathrm{H2E}} \quad \text{(D.26)}$$

Hydrogen boiler. Heat generation constraint:

$$\left(H_{\mathrm{2,H2E,H2B}}(t) + H_{\mathrm{2,H2S,H2B}}(t)\right)\cdot\eta_{\mathrm{H2B}} = H_{\mathrm{H2B,process}}(t) \quad \text{(D.27)}$$

Sizing constraint:

$$H_{\mathrm{H2B,process}}(t) \le s_{\mathrm{H2B}} \quad \text{(D.28)}$$

Battery. State of energy:

$$SOE_{\mathrm{bat}}(t) = \begin{cases} 0, & \text{if } t = 0 \\ SOE_{\mathrm{bat}}(t-1) + \\ \eta_{\mathrm{bat}}\cdot\Delta t\cdot\left(P_{\mathrm{gr,bat}}(t-1) + P_{\mathrm{CHP,bat}}(t-1)\right) - \\ \frac{1}{\eta_{\mathrm{bat}}}\cdot\Delta t\cdot\left(P_{\mathrm{bat,process}}(t-1) + P_{\mathrm{bat,ElB}}(t-1) + P_{\mathrm{bat,HP}}(t-1) + \right. \\ \left. P_{\mathrm{bat,H2E}}(t-1) + P_{\mathrm{bat,gr}}(t-1)\right), & \text{otherwise} \end{cases}$$

Maximum charge constraint:

$$P_{\mathrm{gr,bat}}(t) + P_{\mathrm{GT,bat}}(t) \le \frac{s_{\mathrm{bat}}}{\eta_{\mathrm{bat}}}\cdot\frac{\mathrm{crate}_{\mathrm{bat}}}{\Delta t}\cdot b_1(t) \quad \text{(D.29)}$$

Maximum discharge constraint: Discharging for $t = 0$:

$$P_{\mathrm{bat,process}}(0) + P_{\mathrm{bat,ElB}}(0) + P_{\mathrm{bat,HP}} + P_{\mathrm{bat,H2E}}(0) + P_{\mathrm{bat,gr}}(0) = 0 \quad \text{(D.30)}$$

Discharging for $t > 0$:

$$P_{\mathrm{bat,process}}(t) + P_{\mathrm{bat,ElB}}(t) + P_{\mathrm{bat,HP}}(t) + P_{\mathrm{bat,H2E}}(t) + P_{\mathrm{bat,gr}}(t) \le s_{\mathrm{bat}}\cdot\eta_{\mathrm{bat}}\cdot\frac{\mathrm{crate}_{\mathrm{bat}}}{\Delta t}\cdot(1 - b_1(t)) \quad \text{(D.31)}$$

Sizing constraint:

$$SOE_{\mathrm{bat}}(t) \le s_{\mathrm{bat}} \quad \text{(D.32)}$$

Thermal energy storage. State of energy (SOE):

$$SOE_{\mathrm{TES}}(t) = \begin{cases} 0, & \text{if } t = 0 \\ SOE_{\mathrm{TES}}(t-1) + \\ \left(H_{\mathrm{CHP,TES}}(t-1) + H_{\mathrm{ElB,TES}}(t-1) + H_{\mathrm{HP,TES}}(t-1)\right)\cdot\Delta t - \\ \frac{H_{\mathrm{TES,process}}(t-1)}{\eta_{\mathrm{TES}}}\cdot\Delta t, & \text{otherwise} \end{cases} \quad \text{(D.33)}$$

Maximum charge constraint

$$H_{\mathrm{CHP,TES}}(t) + H_{\mathrm{ElB,TES}}(t) + H_{\mathrm{HP,TES}}(t) \le \frac{s_{\mathrm{TES}}\cdot\mathrm{crate}_{\mathrm{TES}}}{\Delta t}\cdot b_2(t) \quad \text{(D.34)}$$

Maximum discharge constraint: Discharging for $t = 0$:

$$H_{\mathrm{TES,process}}(0) = 0 \quad \text{(D.35)}$$

Discharging for $t > 0$:

$$H_{\mathrm{TES,process}}(t) \le \frac{s_{\mathrm{TES}}\cdot\eta_{\mathrm{TES}}\cdot\mathrm{crate}_{\mathrm{TES}}}{\Delta t}\cdot(1 - b_2(t)) \quad \text{(D.36)}$$

Sizing constraint:

$$SOE_{\mathrm{TES}}(t) \le s_{\mathrm{TES}} \quad \text{(D.37)}$$

Hydrogen storage. State of energy:

$$SOE_{\mathrm{H2S}}(t) = \begin{cases} 0, & \text{if } t = 0 \\ SOE_{\mathrm{H2S}}(t-1) + \left(H_{\mathrm{2,H2E,H2S}}(t-1) - \frac{H_{\mathrm{2,H2S,H2B}}(t-1)}{\eta_{\mathrm{H2S}}}\right)\cdot\Delta t, & \text{otherwise} \end{cases} \quad \text{(D.38)}$$

Charge constraint

$$H_{\mathrm{2,H2E,H2S}}(t) \le s_{\mathrm{H2S}}\cdot b_3(t) \quad \text{(D.39)}$$

Discharge constraint: Discharging for $t = 0$:

$$H_{\mathrm{2,H2S,H2B}}(0) = 0 \quad \text{(D.40)}$$

Discharging for $t > 0$:

$$H_{\mathrm{2,H2S,H2B}}(t) \le \frac{s_{\mathrm{H2S}}\cdot\eta_{\mathrm{H2S}}}{\Delta t}\cdot(1 - b_3(t)) \quad \text{(D.41)}$$

Sizing constraint:

$$SOE_{\mathrm{H2S}}(t) \le s_{\mathrm{H2S}} \quad \text{(D.42)}$$

Grid connection capacity. Maximum inflow constraint:

$$\mathrm{cap}_{\mathrm{gr}}\cdot b_4(t) \ge P_{\mathrm{gr,process}}(t) + P_{\mathrm{gr,ElB}}(t) + P_{\mathrm{gr,bat}}(t) + P_{\mathrm{gr,HP}}(t) + P_{\mathrm{gr,H2E}}(t) \quad \text{(D.43)}$$

Maximum outflow constraint:

$$P_{\mathrm{GT,gr}}(t) + P_{\mathrm{bat,gr}}(t) \le \mathrm{cap}_{\mathrm{gr}}\cdot(1 - b_4(t)) \quad \text{(D.44)}$$

Data availability

The code, selected input data and all results are going to be uploaded to a 4TU repository (DOI: 10.4121/3badc1a4-a0ac-4560-8e1e-2355214331fe) and a GitHub repository (https://github.com/SvenjaBie/ElectrUtilPapInd_Open) once the article is ready for publication. They can be shared earlier upon request.

References

[1] UNFCCC. The paris agreement. Tech report, 2016, URL https://treaties.un.org/Pages/ViewDetails.aspx?src=TREATY&mtdsg_n=XXVII-7-.

[2] Ministry of the Energy Transition. European overview of GHG emissions. 2023, URL https://www.statistiques.developpement-durable.gouv.fr/edition-numerique/chiffres-cles-du-climat-2023/en/credits.

[3] International Energy Agency. Renewable energy for industry from green energy to green materials and fuels. Tech report, 2017, URL www.iea.org/t&c/.

[4] Roelofsen Occo, Somers Ken, Speelman Eveline, Witteveen Maaike. Plugging in: What electrification can do for industry. Tech report, McKinsey & Company; 2020.

[5] Son Hyunsoo, Kim Miae, Kim Jin Kuk. Sustainable process integration of electrification technologies with industrial energy systems. Energy 2022;239. http://dx.doi.org/10.1016/j.energy.2021.122060.

[6] Wei Max, McMillan Colin A, de la Rue du Can Stephane. Electrification of Industry: Potential, Challenges and Outlook. In: Current sustainable/renewable energy reports. 6, (4):2019, p. 140–8. http://dx.doi.org/10.1007/s40518-019-00136-1.

[7] Zühlsdorf Benjamin. IEA high-temperature heat pumps task 1-technologies task report operating agent, Tech report. URL https://heatpumpingtechnologies.org/annex58/wp-content/uploads/sites/70/2023/09/annex-58-task-1-technologies-task-report.pdf.

[8] Padullés Roger, Hansen Magnus Lyck, Andersen Martin Pihl, Zühlsdorf Benjamin, Jensen Jonas Kjæ r, Elmegaard Brian. Optimal operation of industrial heat pumps with stratified thermal energy storage for emissions and cost reduction using day-ahead predictions. Appl Therm Eng 2025;266:125703. http://dx.doi.org/10.1016/j.applthermaleng.2025.125703, URL https://linkinghub.elsevier.com/retrieve/pii/S1359431125002947.

[9] Wiertzema Holger, Svensson Elin, Harvey Simon. Bottom–Up Assessment Framework for Electrification Options in Energy-Intensive Process Industries. Front Energy Res 2020;8. http://dx.doi.org/10.3389/fenrg.2020.00192.

[10] Kim Jin-Kuk. e-Site Analysis: Process Design of Site Utility Systems With Electrification for Process Industries. Front Therm Eng 2022;2. http://dx.doi.org/10.3389/fther.2022.861882.

[11] Walden Jasper VM, Stathopoulos Panagiotis. The impact of heat pump load flexibility on its process integration and economics. J Clean Prod 2024;462. http://dx.doi.org/10.1016/j.jclepro.2024.142643.

[12] Walden Jasper VM, Bähr Martin, Glade Anselm, Gollasch Jens, Tran A Phong, Lorenz Tom. Nonlinear operational optimization of an industrial power-to-heat system with a high temperature heat pump, a thermal energy storage and wind energy. Appl Energy 2023;344. http://dx.doi.org/10.1016/j.apenergy.2023.121247.

[13] Trevisan Silvia, Buchbjerg Bjarke, Guedez Rafael. Power-to-heat for the industrial sector: Techno-economic assessment of a molten salt-based solution. Energy Convers Manage 2022;272. http://dx.doi.org/10.1016/j.enconman.2022.116362.

[14] Baumgärtner Nils, Delorme Roman, Hennen Maike, Bardow André. Design of low-carbon utility systems: Exploiting time-dependent grid emissions for climate-friendly demand-side management. Appl Energy 2019;247:755–65. http://dx.doi.org/10.1016/j.apenergy.2019.04.029.

[15] Reinert Christiane, Schellhas Lars, Frohmann Julia, Nolzen Niklas, Tillmanns Dominik, Baumgärtner Nils, et al. Combining optimization and life cycle assessment: Design of low-carbon multi-energy systems in the SecMOD framework. In: Computer aided chemical engineering, vol. 51, Elsevier B.V.; 2022, p. 1201–6. http://dx.doi.org/10.1016/B978-0-323-95879-0.50201-0.

[16] Bielefeld Svenja, Cvetković Miloš, Ramírez Andrea. The potential for electrifying industrial utility systems in existing chemical plants. Applied Energy 2025;392:125988. http://dx.doi.org/10.1016/j.apenergy.2025.125988, https://www.sciencedirect.com/science/article/pii/S0306261925007184.

[17] Fleschutz Markus, Bohlayer Markus, Braun Marco, Murphy Michael D. From prosumer to flexumer: Case study on the value of flexibility in decarbonizing the multi-energy system of a manufacturing company. Appl Energy 2023;347:121430. http://dx.doi.org/10.1016/j.apenergy.2023.121430.

[18] Oluleye Gbemi, Jobson Megan, Smith Robin. Process integration of waste heat upgrading technologies. Process Saf Environ Prot 2016;103(Part B):315–33. http://dx.doi.org/10.1016/j.psep.2016.02.003.

[19] Van de Bor DM, Infante Ferreira CA. Quick selection of industrial heat pump types including the impact ofthermodynamic losses. Energy 2013;53:312–22. http://dx.doi.org/10.1016/j.energy.2013.02.065.

[20] Voll Philip, Klaffke Carsten, Hennen Maike, Bardow André. Automated superstructure-based synthesis and optimization of distributed energy supply systems. Energy 2013;50(1):374–88. http://dx.doi.org/10.1016/j.energy.2012.10.045.

[21] Madeddu Silvia, Ueckerdt Falko, Pehl Michaja, Peterseim Juergen, Lord Michael, Kumar Karthik Ajith, et al. The CO2reduction potential for the European industry via direct electrification of heat supply (power-to-heat). Environ Res Lett 2020;15(12). http://dx.doi.org/10.1088/1748-9326/abbd02.

[22] Danish Energy Agency. Technology data-energy plants for electricity and district heating generation. Tech report, 2016, URL http://www.ens.dk/teknologikatalog.

[23] Krishnan Subramani, Koning Vinzenz, Theodorus de Groot Matheus, de Groot Arend, Mendoza Paola Granados, Junginger Martin, et al. Present and future cost of alkaline and PEM electrolyser stacks. Int J Hydrog Energy 2023. http://dx.doi.org/10.1016/j.ijhydene.2023.05.031.

[24] Wang Xiaobo, Huang Wentao, Wei Wei, Tai Nengling, Li Ran, Huang Yiwen. Day-Ahead Optimal Economic Dispatching of Integrated Port Energy Systems Considering Hydrogen. IEEE Trans Ind Appl 2022;58(2):2619–29. http://dx.doi.org/10.1109/TIA.2021.3095830.

[25] Yang Huan, Lin Xiaolong, Pan Hejitian, Geng Sajie, Chen Zhengyu, Liu Yinhe. Energy saving analysis and thermal performance evaluation of a hydrogen-enriched natural gas-fired condensing boiler. Int J Hydrog Energy 2023;48(50):19279–96. http://dx.doi.org/10.1016/j.ijhydene.2023.02.027.

[26] Arup, kiwa. Industrial boilers. Study to develop cost and stock assumptions for options to enable or require hydrogen-ready industrial boilers. Tech report, 2022, URL https://assets.publishing.service.gov.uk/government/uploads/system/uploads/attachment_data/file/1123264/External_research_study_hydrogen-ready_industrial_boilers.pdf.

[27] International Renewable Energy Agency. Innovation outlook thermal energy storage. 2020, URL www.irena.org.

[28] NREL. Utility-Scale Battery Storage. 2023, https://www.ldescouncil.com/assets/pdf/221108_NZH_LDES brochure.pdf.

[29] LDES Council, Company McKinsey. Net-zero heat long duration energy storage to accelerate energy system decarbonization contents. Tech report, 2022, URL https://www.ldescouncil.com/assets/pdf/221108_NZH_LDES brochure.pdf.

[30] Petkov Ivalin, Gabrielli Paolo. Power-to-hydrogen as seasonal energy storage: an uncertainty analysis for optimal design of low-carbon multi-energy systems. Appl Energy 2020;274. http://dx.doi.org/10.1016/j.apenergy.2020.115197.

[31] ENTSO-E. ENTSO-E Transparence Platform. URL https://transparency.entsoe.eu/.

[32] investingcom. Dutch TTF Natural Gas Futures Historical Data. URL https://www.investing.com/commodities/dutch-ttf-gas-c1-futures-historical-data.

[33] Ember. Carbon Price Tracker. URL https://ember-climate.org/data/data-tools/carbon-price-viewer/.

[34] ICE. Dutch TTF Natural Gas Futures. URL https://www.ice.com/products/27996665/Dutch-TTF-Natural-Gas-Futures/data?marketId=5815810&span=3.

[35] Statista. Daily European Union Emission Trading System (EU-ETS) carbon pricing from 2022 to 2024 (in euros per metric ton). URL https://www.statista.com/statistics/1322214/carbon-prices-european-union-emission-trading-scheme/.

[36] Towler Gavin, Sinnott Ray. Chemical engineering design: principles, practice and economics of plant and process design. Tech report, 2nd Ed..

[37] BVES. Technology: solid medium heat storage GENERAL DESCRIPTION mode of energy intake and output. Tech report, 2024, URL https://iea-es.org/wp-content/uploads/public/FactSheet_Thermal_Sensible_Solids.pdf.

[38] ISPT. A one- gigawatt green-hydrogen plant. advanced design and total installed-capital costs. Tech report, 2022.

[39] Directorate-General for Financial Stability Financial Services, Capital Markets Union. Corporate sustainability reporting. URL https://finance.ec.europa.eu/capital-markets-union-and-financial-markets/company-reporting-and-auditing/company-reporting/corporate-sustainability-reporting_en.

[40] Sarbu Ioan, Sebarchievici Calin. A comprehensive review of thermal energy storage. In: Sustainability (Switzerland). 10, (1). 2018, http://dx.doi.org/10.3390/su10010191.